Acta Societatis Botanicorum Poloniae

INVITED REVIEW Acta Soc Bot Pol 83(4):423–440 DOI: 10.5586/asbp.2014.037
Received: 2014-11-16 Accepted: 2014-12-10 Published electronically: 2014-12-31

Oxygenic photosynthesis: translation to solar fuel technologies

Julian David Janna Olmos[1], Joanna Kargul[2]*

[1] Faculty of Biology, University of Warsaw, Miecznikowa 1, 02-096 Warsaw, Poland

[2] Centre of New Technologies, University of Warsaw, Banacha 2c, 02-097 Warsaw, Poland (it is the present address of the first author)

Abstract

Mitigation of man-made climate change, rapid depletion of readily available fossil fuel reserves and facing the growing energy demand that faces mankind in the near future drive the rapid development of economically viable, renewable energy production technologies. It is very likely that greenhouse gas emissions will lead to the significant climate change over the next fifty years. World energy consumption has doubled over the last twenty-five years, and is expected to double again in the next quarter of the 21st century. Our biosphere is at the verge of a severe energy crisis that can no longer be overlooked. Solar radiation represents the most abundant source of clean, renewable energy that is readily available for conversion to solar fuels. Developing clean technologies that utilize practically inexhaustible solar energy that reaches our planet and convert it into the high energy density solar fuels provides an attractive solution to resolving the global energy crisis that mankind faces in the not too distant future. Nature's oxygenic photosynthesis is the most fundamental process that has sustained life on Earth for more than 3.5 billion years through conversion of solar energy into energy of chemical bonds captured in biomass, food and fossil fuels. It is this process that has led to evolution of various forms of life as we know them today. Recent advances in imitating the natural process of photosynthesis by developing biohybrid and synthetic "artificial leaves" capable of solar energy conversion into clean fuels and other high value products, as well as advances in the mechanistic and structural aspects of the natural solar energy converters, photosystem I and photosystem II, allow to address the main challenges: how to maximize solar-to-fuel conversion efficiency, and most importantly: how to store the energy efficiently and use it without significant losses. Last but not least, the question of how to make the process of solar energy conversion into fuel not only efficient but also cost effective, therefore attractive to the consumer, should be properly addressed.

Keywords: solar fuels; photosystem I; photosystem II; CO_2; photosynthesis; artificial leaf; artificial photosynthesis; solar-to-fuel nanodevices

Introduction

Finding renewable sources of energy is of paramount importance. It has been estimated that all the fossil fuel reserves are likely to be irreversibly exhausted by 2112 [1,2]. Coal reserves are estimated to be readily available up to 2112, and are likely to be the only fossil fuel remaining after 2042 [1]. Total global energy demand could rise by up to 80% by mid-21st century from its level in 2000 [3]. Sunlight, on the other hand, is by all means an infinite, inexhaustible and gargantuan source of energy. The power of 1 hour of solar energy reaching our planet is equivalent to the current annual global energy consumption of approximately 16.3 TW [4]. Crops, grasses, trees, cyanobacteria and algae capture solar energy via their photosynthetic machinery and store it in a wide range of feedstock in the form of chemical bonds (i.e., sugars, lipids and starch). The earliest form of photosynthesis is estimated to have evolved circa 3.5 billion years ago, occurring in an environment of low atmospheric oxygen and in the presence of high levels of reducing molecules including methane, hydrogen gas, hydrogen sulfide and other organic compounds which were all employed as the reducing agents necessary for anoxygenic photosynthesis [5]. As the reducing atmosphere was depleted over time, the need for using water as the source of reducing equivalents placed a mandatory selection pressure leading to the evolution of oxygenic photosynthesis where oxidation occurred by extracting hydrogen from water. The evolution of the water splitting reaction gave rise to oxygenic photosynthesis, whereby oxygen is produced as a by-product of water photo-oxidation. The first organisms to engage in such biologically revolutionary process were (proto)cyanobacteria, which are thought to have evolved from primitive anoxic photosynthetic bacteria [6].

* Corresponding author. Email: j.kargul@uw.edu.pl

Handling Editor: Beata Zagórska-Marek

Evolution of photosynthesis

It has been well established that photosynthetic organisms have transformed life on earth by their inherent ability to perform solar energy conversion. The earliest phototrophs were almost certainly non-oxygenic, and it is now known that photosynthesis evolved early in geological history of the Earth, in the early Archean eon circa 3.5 billion years ago. The enzymatic and energetic fundamentals of life were revolutionized approximately 2.4 billion years ago by the Great Oxidation Event, i.e., the rise of atmospheric oxygen due to oxygenic photosynthesis. The onset of oxygenic photosynthesis is often referred to as the "Big Bang of evolution" [7] as it drove evolutionary events in Earth's history on an unprecedented scale including appearance of aerobic respiration and colonization of terrestrial ecosystems by multicellular organisms due to the formation of the protective ozone layer. In parallel, development of the new photosynthetic pathways occurred through the modification of existing and alternative ways of carbon fixation. Phototrophs evolved further by means of lateral gene transfer leading to formation of the basic photosynthetic components, namely the photosynthetic reaction centers (RCs) as well as by some endosymbiotic events. Various types of evidence obtained from biochemical, physiological and biophysical studies of photosynthetic complexes together with comparative genomics data show a very rich complexity of photosynthetic features. At the same time, discovery of evolutionary similarity of structural features of the main photosynthetic components has allowed to formulate some hypotheses on the origin and evolution of photosynthesis, as overviewed below.

Molecular evolution occurs through DNA alterations (typically mutations) that create new proteins that offer alternative metabolic opportunities [8]. The building blocks for molecular innovation may be provided by an organism, gene or genome duplication [9,10]. It is thought that gene duplication, modification and divergence gave birth to the evolution of photosynthetic RCs (see [5] and references therein). It has been postulated that a single gene, which coded for a homodimeric protein, was duplicated subsequently to produce heterodimeric RCs. The mechanisms behind the evolution of the fused RC core and antennae in some species of higher plants and algae could be explained by gene fusion and splitting. On the other hand, the transfer of metabolic capacities between different organisms most likely occurred by lateral gene transfer [11] and could also explain the presently observed plethora of photosynthetic light-harvesting complexes (LHCs) associated with RCs that evolved in different families of phototrophs. As a matter of fact, certain genomes include gene clusters which themselves contain RC-coding genes together with certain photosynthetic pigments biosynthesis pathways [12], which most certainly provided the genetic platform for lateral transfer of photosynthetic traits between species.

Numerous structural, spectroscopic, thermodynamic, molecular sequence and genetic studies provided molecular evidence supporting the hypothesis that all RCs have evolved from a common ancestor and have been optimized so as to maximize the efficiency of solar energy conversion [5]. In all cases of various types of RCs, the fundamental mechanistic principle is to achieve energy storage by ultrafast separation of the primary electron donors and acceptors during the primary charge transfer, thus avoid wasteful recombination reactions. This is achieved by optimal arrangement of the electron transport cofactors within the protein "smart matrix" of the RCs. However, it should be pointed out that the reversibility of charge separation (i.e. fast charge recombination processes) has also been demonstrated for various types of photosynthetic RCs (e.g., for photosystem I and photosystem II, PSI and PSII) as the regulatory mechanism for effective excitation quenching by closed (oxidized) RCs. The extent of this reversibility depends on the amount of free energy associated with the charge-separated state, which can be modulated by various modes of excitation dynamics that exist within the RCs and the associated antennae.

X-ray crystallographic analyses of photosynthetic RCs demonstrated that a three-dimensional protein and cofactor structure of RCs is remarkably conserved, despite only minimal amino acid sequence identity [5,13]. Two types of photosynthetic RCs can be distinguished depending on the type of the primary electron acceptor. These are type I and type II RCs which employ either (bacterio)chlorophyll (Chl) or (bacterio)pheophytin as the primary acceptor, respectively. Type I RCs are present in green sulfur bacteria and heliobacteria, while purple photosynthetic bacteria and green filamentous, non-sulfur bacteria have all type II RCs. In cyanobacteria, algae and higher plants one RC of each type is present, i.e., PSI (type I RC) and PSII (type II RC). These work in tandem to drive oxygenic photosynthesis using water as the primary source of reducing equivalents for subsequent reduction of CO_2 into sugars.

The common design scheme in all photosynthetic RCs is the charge-separation cofactor assembly that is bound within a protein dimer composed of 5-trans-membrane (TM) domain subunits. Each half of this common dimeric RC unit contains a nearly identical set of cofactors. The arrangements of these cofactors exhibit minimal variation in all the available crystal structures of RCs [5]. X-ray crystallographic studies revealed that all RCs are characterized by a pseudo-2 fold symmetry axis that relates both the cofactors and their protein scaffold. In cyanobacteria and eukaryotic phototrophs, the D1/D2 heterodimer of PSII RC, is flanked by two closely related 6-TM inner antenna complexes, CP43 and CP47 that both harbor additional core antenna pigments. These 6-TM antenna subunits are evolutionarily related to the N-terminal part of the type I RC, which forms the core antenna [14]. In contrast to the cyanobacterial type II RC of PSII in which 5 TMs and 6 TMs are separate proteins, all known type I RCs are 11-TM dimers, which consist of the C-terminal 5-TM RC complex and the N-terminal 6-TM core antenna, all of which belong to a single protein. In green sulfur bacteria and heliobacteria, type I RCs are homodimeric, whereas cyanobacterial, algal and higher plant type I RC represented by PSI is heterodimeric, not only structurally but also functionally, as the two electron transport branches that exist within the RC PsaA/PsaB heterodimer also exhibit different kinetic characteristics [5].

Primary photosynthetic events: unparalleled efficiency

As discussed above, oxygenic photosynthesis represents the major process of solar energy conversion on Earth today. Most significantly, this is without a doubt the most important process for the input of organic energy into the biosphere: thermal, radioactive and chemical inputs being by comparison negligible. Unfortunately, photosynthesis as an overall process is rather inefficient. Massive losses in light absorption, transmission, reflection, and scattering, as well as losses of absorbed photon energy as heat limit the energy storage in biomass to a mere 5–7% (as an upper limit) for plants and algae, with an average of 0.2% [15], as shown in Fig. 1.

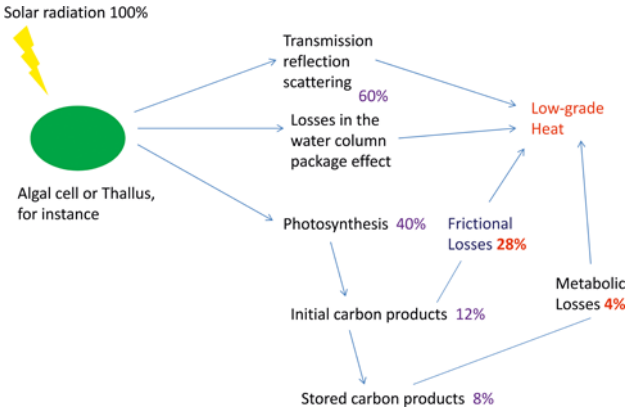

Fig. 1 Energy losses and dissipation in photosynthesis. Much of the incident energy is lost as low-grade heat either directly or indirectly. Only a small amount of energy is stored as chemical free energy in new organic material. Adapted from Larkum [95].

Taking most factors into consideration, including the light absorption processes, trans-membrane electron/proton transport and any losses due to radiative and non-radiative dissipation the overall energy conversion efficiency decreases from the primary photosynthetic light capture and charge separation events (up to 95%) to mere 30% for the process of the Calvin–Benson cycle [16]. In terms of efficiency of solar energy conversion, the rates of the even best crop plants are less than 1% [17]. It is then unsurprising that scientists have invested considerable time and resources to study the structure and function of the primary solar energy converters, PSII and PSI which both exhibit remarkably high power conversion efficiencies. The first molecular steps of photosynthesis, the so-called light reactions, work at an impressive quantum yield close to unity, and no man-made energy-converting device can reach such a remarkable efficiency. At low-to-medium light levels PSII and PSI operate at a quantum efficiency of above 95% [18]. Quantum yield of PSI is particularly impressive at unity, making it an almost perfect Einstein photoelectric device. It is then obvious that in order to maximize the solar energy conversion efficiency for production of solar fuels we must short-circuit the photosynthetic energy conversion processes and use directly the reducing equivalents generated through the primary photosynthetic events, without proceeding to generation of biomass where the most significant energy losses occur (see Fig. 2).

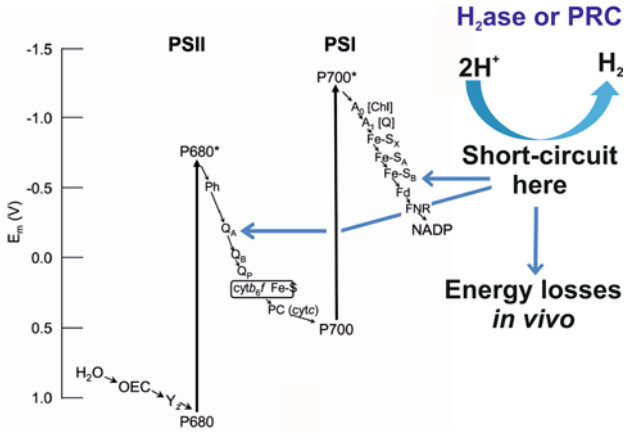

Fig. 2 Short-circuiting the light reactions to maximize power conversion efficiency and minimize energy losses. The dark reactions of photosynthesis are energetically expensive, leading to the loss of energy conversion efficiency. Short-circuiting of primary photosynthetic event for proton reduction and photocatalysis may considerably enhance solar-to-fuel conversion efficiency. PSI and PSII can be short-circuited at the terminal F_B cluster ([18] and references therein) or the Q_A site ([96] and references therein), respectively.

PSI and PSII capture quanta of solar light which are transferred to specialized pairs of chlorophyll (Chl) *a* molecules forming the photochemical RCs, P700 and P680, respectively. Upon capture of solar light PSII and PSI work in tandem to generate vectorial electron flow (with water molecules as the primary source of electrons and protons), as well as forming the trans-membrane proton gradient across the thylakoid membrane through the action of the third macromolecular protein complex also embedded in the thylakoid membranes between PSII and PSI, cytochrome b_6f. The electromotive force of proton gradient powers the thylakoid-bound ATP synthase to produce ATP and enables reduction of NADP, being the final recipient of photogenerated electrons (see Fig. 3).

In a different route of electron flow, directed mainly around PSI, electrons may be reused from either NADPH to plastoquinone or reduced ferredoxin, and subsequently to the cytochrome b_6f complex [19–21]. A pH gradient is generated by such cyclic electron flow, leading to formation of exclusively ATP without accumulation of the reduced NADP (NADPH). The precise physiological role of cyclic electron flow around PSI is still somewhat controversial, but it is known that in higher plants this type of photosynthetic electron flow consists of two partially redundant pathways, i.e., NADPH dehydrogenase (NDH)- and PGRL1/PGR5-dependent pathways, both of which are fuelled with electrons from reduced ferredoxin [22–24]. Recently, it has been shown that cyclic electron flow is important for regulation of the photosynthetic yield, under various stress and metabolic conditions (e.g., [25,26]).

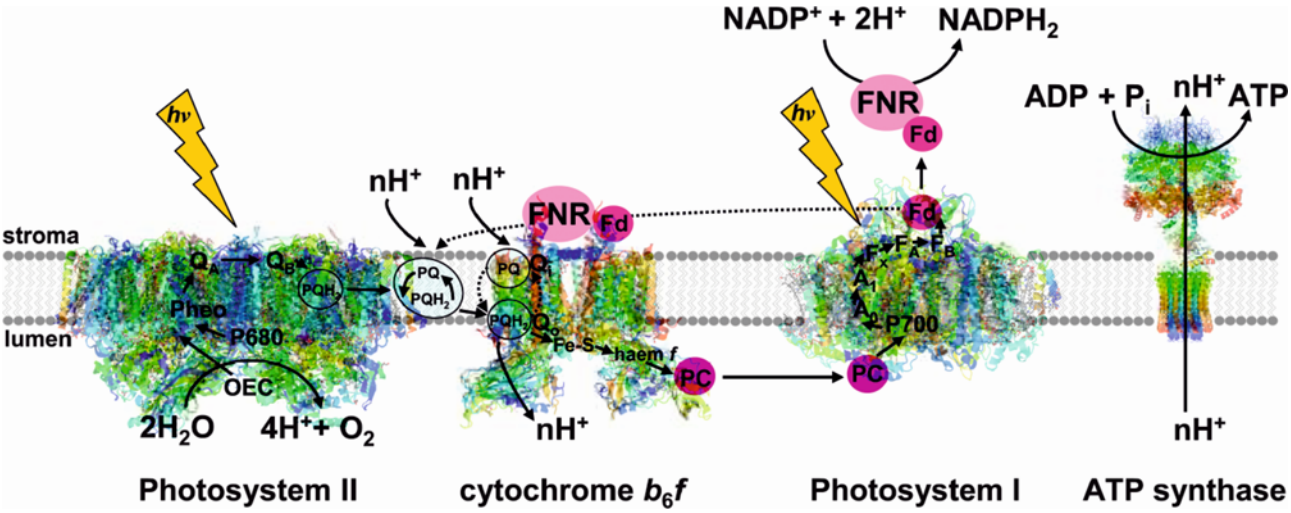

Fig. 3 Structural representation of the linear photosynthetic electron transfer path in higher plants. X-ray crystal structures of major protein complexes are highlighted, photosystem II (3ARC), cytochrome b_6f (1VF5), and photosystem I (1JB0), and their arrangement in the thylakoid membrane in order to conduct a linear photosynthetic electron transport and generate reducing equivalents and NADPH. The proton gradient generated powers ATP production by proton transport via the ATP synthase. Both ATP and NADPH are employed for fixation and reduction of CO_2 into carbohydrates. The OEC (oxygen evolving complex) is indicated by an arrow, and is comprised of a Mn_4CaO_5 cluster (see body of the text) which oxidizes substrate water molecules. Pheo – pheophytin: a primary electron acceptor; Q_A, Q_B – primary and secondary quinone electron acceptors; PQ/PQH_2 – plastoquinone/plastoquinol: oxidized and reduced plastoquinone; PC – plastocyanin; A_0 – Chl*a*; A_1 – phylloquinione; F_x, F_A, F_B – [4Fe-4S] clusters; Fd – ferredoxin; FNR – ferredoxin: NADP reductase. Under certain metabolic ATP-depleted conditions, cyclic electron flow is induced (dotted arrow) which generates ATP without production of NADPH. Adapted from Kargul and Barber [5].

Water splitting at the oxygen-evolving center of photosystem II

PSII is the molecular nanomachine responsible for generation of oxygenic life on Earth through its catalytic activity of water photooxidation. Whilst most other photosynthetic type II RCs use small organic molecules as electron donors, the presence of the oxygen-evolving center (OEC) in close proximity to the P680 photochemical RC ingeniously permits for the use of H_2O as the electron donor [27,28]. The Mn_4CaO_5 cluster of the OEC contains a Mn_3CaO_4 distorted cubane structure, in which with three Mn atoms and one Ca cation occupy four corners, whilst the four O atoms occupy the other corners (see Fig. 4, inset) [29]. The fourth Mn ion (Mn4 or the "dangler" Mn) is covalently linked to the cubane by a di-μ-oxo bridge involving the O5 and O4 atoms of the cubane [29]. The metals within the cluster are surrounded by a number of amino acid residues, of which seven (mostly originated from the D1 subunit) provide the direct ligands to the metals through their carboxylate groups in a monodentate or bidentate mode [29]. Importantly, the latest near-atomic (1.9 Å) X-ray crystal structure of PSII purified from a cyanobacterium *Thermosynechococcus vulcanus* provides the first direct evidence on the location of the primary water substrate molecules which are believed to be coordinated to both the Ca ion and the dangler Mn [29]. The detailed mechanism of water oxidation, especially the formation of molecular oxygen, remains hotly debated, but high-valent Mn species are almost certainly involved in the activation of oxo-ligands to form O-O bond during the water oxidation cycle [28,30].

The process of water splitting requires overall two water molecules and yields four electrons, four protons, and one molecule of O_2. The process, which requires capture of four subsequent photons in the P680 RC, involves the charge separated states and the consequent accumulation of 4 positive holes on the OEC which are then reduced with 4 electrons derived from 2 substrate water molecules. PSII has been estimated to conduct the water splitting reaction at a turnover frequency (TOF) of 300 s^{-1} in vivo [31]. The overall structure of the OEC catalytic site and the mechanistic knowledge that has been superbly advanced by the latest achievements of PSII crystallography greatly inspires a quest for the development of synthetic catalysts for mimicking the energetically demanding water splitting reaction in artificial photoelectrochemical systems to generate solar fuels (as discussed below) at a minimal overpotential, as does PSII.

Reducing power of photosystem I

Upon absorption of red photons by P700 RC of PSI (E_m +0.43 eV) composed of 2 Chl*a* molecules, the highly reducing excited state P700* is formed (E_m –1.3 eV), which then rapidly undergoes oxidization to $P700^+$ followed by electron transfer by the conserved redox cofactors system involving 4 additional Chl*a* molecules, 2 phylloquinones and 3 iron-sulfur [4Fe-4S] clusters. The final electron acceptor, F_B is formed by the iron-sulfur cluster coordinated by the Cys residues of PsaC subunit on the acceptor side of PSI. Reduction of a positive hole $P700^+$ on the donor side of PSI occurs through the specific interaction with the mobile electron carriers, plastocyanin or cytochrome c_6. The potential difference between the primary electron donor P700* and the terminal electron acceptor F_B^- is about 1 V, corresponding to a thermodynamic efficiency of nearly 60% [32].

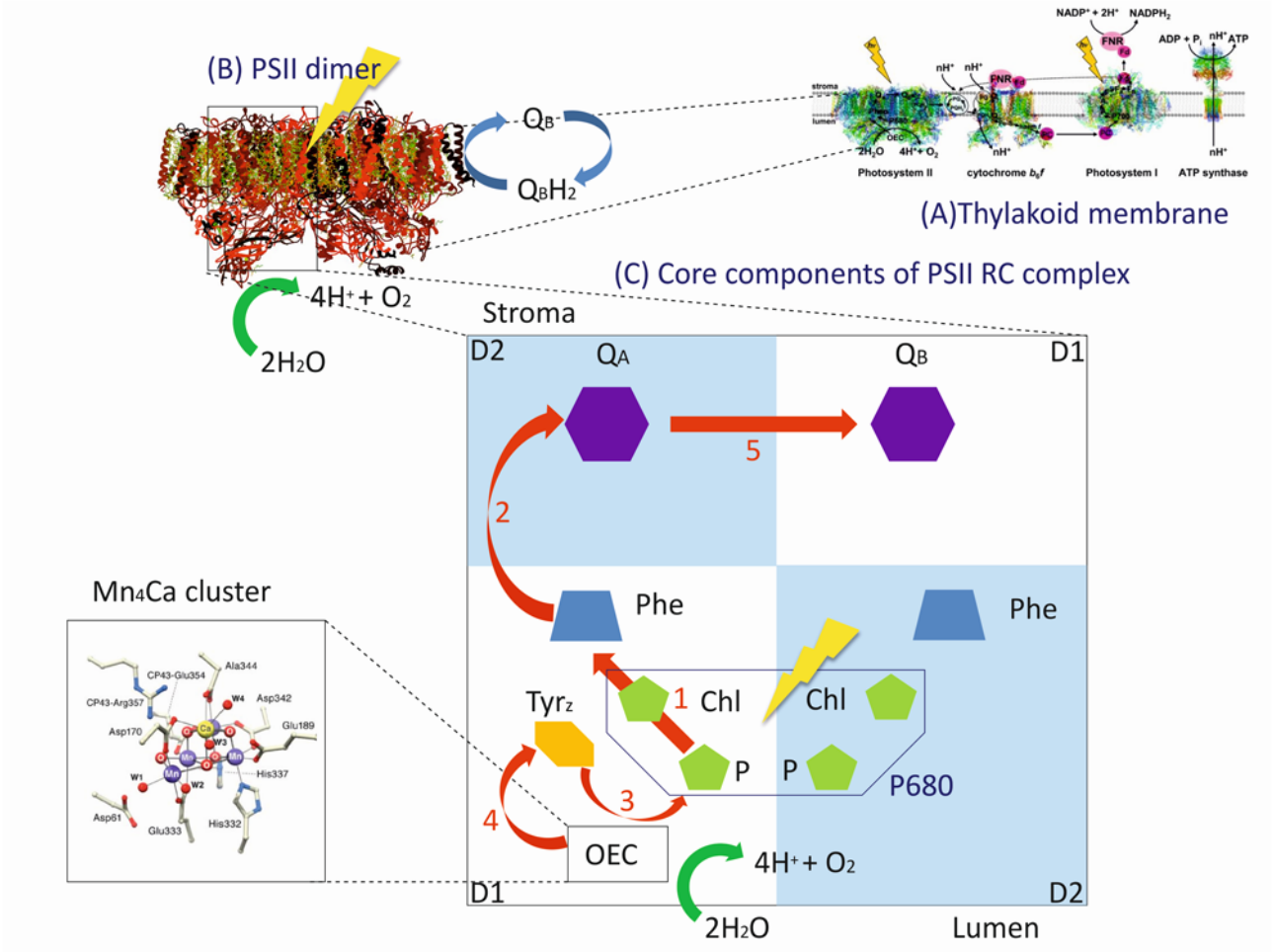

Fig. 4 From structure to function of photosystem II. **a** Structural representation of the linear photosynthetic electron transfer path in the thylakoid membrane. **b** 1.9 Å crystal structure of PSII dimer from *Thermosynechococcus vulcanus* (PDB: 3ARC) [29]. Water splitting at the OEC results in the release of H^+, e^- and O_2, concomitant with the double reduction of the terminal quinone, Q_B, in the Q_B pocket to liberate doubly reduced PQ (PQH_2, plastoquinol) into the thylakoid space. **c** Diagrammatic representation of the electron transfer cofactor arrangement within the RC D1/D2 dimer. Red arrows indicate the direction of the forward electron transfer. Step 1: photoexcitation leads to formation of the charge separated state $P680^+Phe_{D1}^-$. Step 2: transfer of electrons from Phe_{D1}^- to Q_A. Step 3: the positive hole of $P680^+$ is filled by an electron from Tyr_z. Step 4: hole migration from Tyr_z^+ to the Mn_4CaO_5 cluster. Step 5: electron transfer from Q_A^- to the terminal acceptor Q_B. Insert: the latest structure of Mn_4CaO_5 cluster together with coordinating ligands at 1.9 Å [29].

Despite structural complexity (12–17 protein subunits and 127–178 cofactors for the cyanobacterial and higher plant PSI [33–35], PSI operates with a quantum yield of unity and so far, no artificial system gained such a remarkable efficiency. As a consequence, this robust and highly abundant photoactive protein complex constitutes the favorite biological component for construction of the biohybrid photovoltaic (PV) and photoelectrochemical (PEC) devices ([18,36] and references therein). Due to an exceptionally long-lived charge-separated state $P700^+F_B^-$ (~60 ms) and exceptionally low redox potential of the F_B cluster (E_m −0.58 eV), PSI in principle generates sufficient driving force to reduce protons to H_2 at neutral pH [18,37]. As PSI is capable of being both an acceptor ($P700^+$) and a donor (F_B^-) of electrons, this complex has been used in semi-artificial assemblies for generation of both anodic and cathodic photocurrents, as well as solar fuels [18,36,37].

Photosynthesis and reduction of carbon footprint

Microalgae-based technologies to reduce carbon footprint

The term "carbon footprint" has evolved as an important measure of greenhouse gas intensity for diverse activities and products. The carbon footprint is perhaps best expressed as the amount of greenhouse gasses (primarily CO_2) that is produced per capita [38]. The most advanced industrial societies can have enormous values, such as 19–22 tons per capita for the USA, and even more elevated for a few small Arab and European nations, and can be as low to 0.1 or even less for non-industrial nations (e.g., Ethiopia and Somalia). In the light of proven anthropogenic climate change it is important to consider lowering the contribution of various sources towards carbon footprint per capita, particularly for the modern economies which are predominantly powered by burning fossil fuels. This fact places our biosphere in a

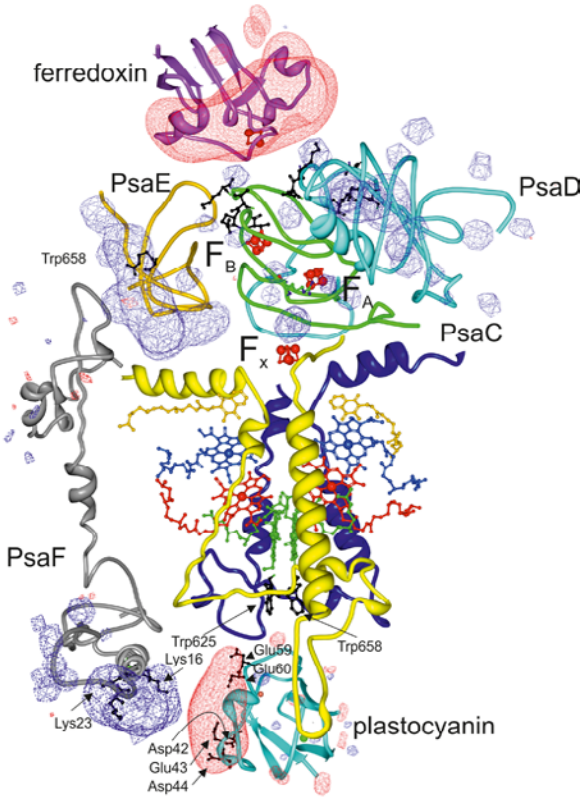

Fig. 5 Electron transport chain in PSI. Depicted are 2 branches of electron transfer cofactors including P700 primary electron donor Chls (green), accessory Chls (red), primary electron acceptor Chls (blue), secondary electron acceptor phylloquinones (yellow) and 3 [4Fe-4S] clusters, F_X, F_A and F_B (red balls). Interaction domains between PSI and plastocyanin and ferredoxin including critical amino acid residues are also shown. Positively and negatively charged regions are colored in as blue and red mesh, respectively. Coordinates are: 3LW5 [35] for PSI, 2PLT for plastocyanin [97] and 3AV8 for ferredoxin [98]. Reproduced with permission from Kargul et al. [18].

precarious situation: not only are our fuel reserves being irreversibly depleted but also man-made climate changes have been altering our biosphere on the scale that is only beginning to be fully comprehended. For these reasons, CO_2 capture and utilization, a concept of turning a greenhouse gas into a useful feedstock, has gained much attention in recent years [39].

Microalgae-based CO_2 photosynthetic fixation is regarded as a potential way to not only reduce CO_2 emission but also achieve energy utilization within microalgal biomass (Fig. 6). However, in this approach culture processing of microalgae plays an important role as it is directly related to the mechanism of microalgal CO_2 fixation and characteristics of microalgal biomass production [40]. According to the capture mechanism, post-combustion CO_2 capture methods can be roughly categorized as chemical absorption, physicochemical adsorption, membrane filtration, cryogenics, chemical looping combustion and biotechnology (e.g., with the use of hydroponic algae or terrestrial vegetations). From a technical point of view all of these methods are feasible in spite of the differences in CO_2 capture efficiency and capture capability of various microalgae.

An alternative feedstock to eukaryotic microalgae is cyanobacteria. The simpler structure of cyanobacteria allows them to be more efficient at carbon fixation from the atmosphere than eukaryotic algae [41]. However, they yield a much smaller photosynthetic conversion efficiency compared to algae [42]. Regardless, cyanobacteria are still being investigated for their inorganic carbon fixation capabilities as they possess a much simpler genetic make-up which can be easily engineered for an enhanced biomass yield, RuBisCO's increased affinity for CO_2 and production of high value products (HVPs) [43–45]. Moreover, several model cyanobacterial species have their genomes fully sequenced. The latter, combined with the fact that genetic manipulation of cyanobacteria is well established allowed for application of high throughput systems biology approaches to engineer cyanobacterial strains producing HVPs [41–46].

Soybean, sesame seeds, wheat, sunflower, switchgrass, rapeseed and peanuts comprise the most common feedstocks used in the first and second generations of biofuels. Moreover, different liquid fuels such as vegetable oil and alcohols (ethanol, propanol and butanol) are generated from these sources. Unfortunately, the competition with arable land for food production is the major limitation of these energy crops. To overcome this limitation, the so-called "third generation" feedstock is postulated to use non-food biomass sources for energy generation [46]. Cyanobacteria are the most promising candidates for the production of such HVPs including biofuels for the following reasons: (***i***) they contain a significant amount of lipids, present mostly in the thylakoid membranes, (***ii***) their photosynthetic and growth rates are higher than those of algae and higher plants, (***iii***) they grow easily and with addition of minimum amount of nutrients and water, employing light as the only energy source for many strains, (***iv***) cultivation is simple and inexpensive.

High value products as a route for carbon footprint reduction

BIOHYDROGEN. Hydrogen gas combustion produces only water as a side product. Hydrogen combustion has an extremely low enthalpy of combustion, at −286 kJ/mol. Moreover, combustion of hydrogen gas releases 572 kJ of energy. This is quite impressive, thermodynamically speaking. Hydrogen, by far, has the highest energetic value of all HVPs [47]. The reversible activity of hydrogenases allows many strains of cyanobacteria to produce hydrogen, often termed the "green fuel". H_2 may be formed as a by-product of N_2 fixation by nitrogenases when cyanobacteria are exposed to N_2 starvation [47]. Additionally, non-heterocystous cyanobacteria seem to be less efficient in H_2 production than heterocystous organisms. Several excellent reviews have reported cyanobacterial species capable of evolving H_2 gas due to the activity of chloroplast reversible hydrogenase that is directly coupled to the linear photosynthetic electron flow [47–49]. One of the problems of employing cyanobacteria (and some hydrogen producing green algae, such as *Chlamydomonas reinhardtii*) is that the most active hydrogenases responsible for H_2 production (Fe-Fe hydrogenases) are irreversibly poisoned by O_2 inherently evolved during photosynthetic light reactions. Moreover, the availability of reducing agents such as NADPH and ferredoxin is an additional limitation as these compounds are also involved

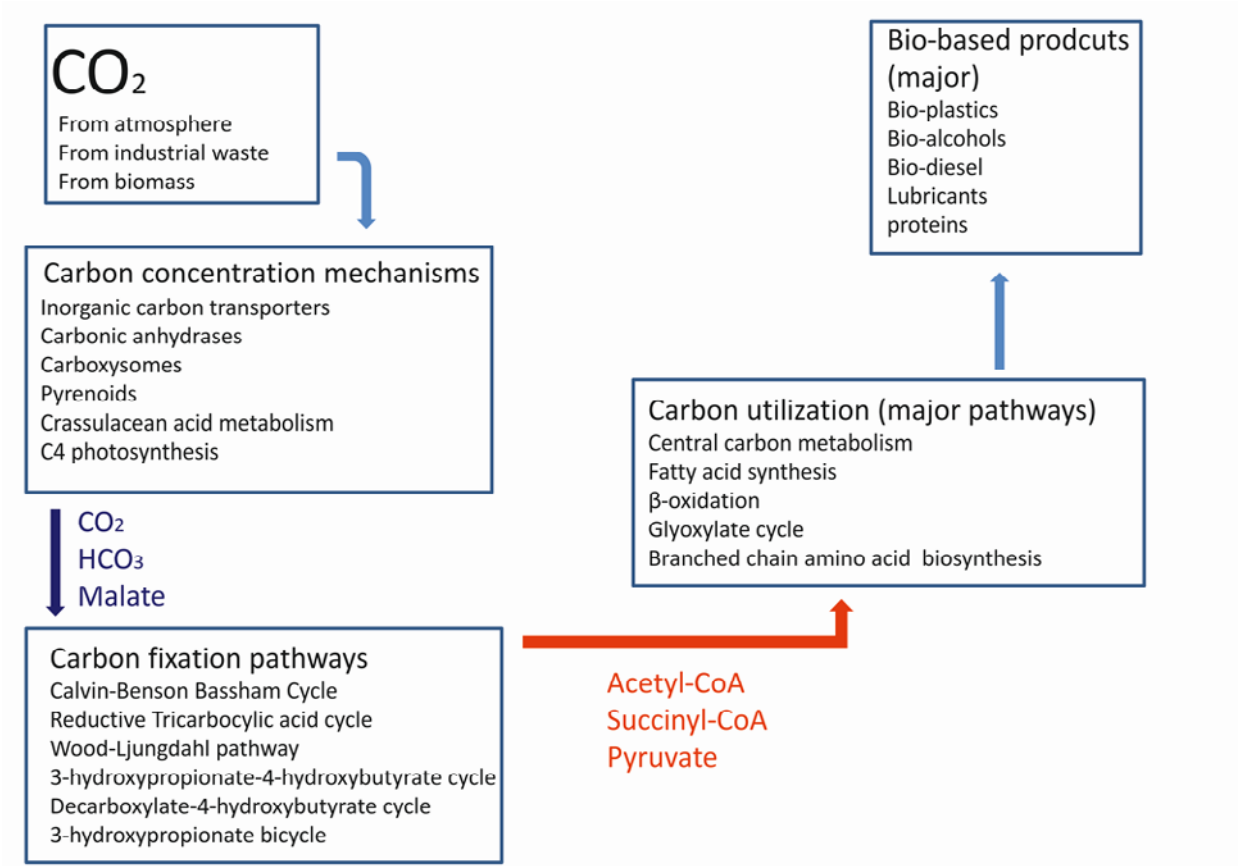

Fig. 6 Carbon concentrating mechanisms, carbon fixation pathways and carbon utilization strategies adopted by various autotrophic organisms, leading to bio-based products. Photosynthetic organisms (cyanobacteria, algae and higher plants) are the main but not exclusive autotrophs that are capable of CO_2 assimilation through the photosynthetic dark reactions. Research on autotrophic bacteria over the last decade showed that these CO_2-utilizing microorganisms could also in principle be applied for reducing carbon footprint on an industrial scale. Scheme adapted from Jajesniak et al. [39].

in other competing metabolic pathways, such as respiration. To overcome these problems Anastasios Melis and colleagues have developed a smart strategy for H_2 production in a green alga *C. reinhardtii* by inducing anaerobiosis in the light following sulfur starvation of the cells, which causes reversible PSII inactivation and thus, inhibition of photosynthetic O_2 evolution. Lowering the ratio of photosynthetic rate below oxidative respiration rate induces anaerobiosis in the cells, which is sufficient for the induction of reversible hydrogenase and cellular H_2 production in the light using photogenerated electrons originated from photoreduced ferredoxin [50]. The economic viability of this approach is somewhat limited by a relatively poor yield. Nevertheless, over the last few years a good progress has been made in this field mainly by isolating the specific mutants of *C. reinhardtii* altered in the rate of cyclic electron transport and degree of non-photochemical quenching (fluorescence and heat) that showed an improved yield of solar-to-H_2 conversion upon sulfur deprivation and increased irradiance compared to the pioneering work of Melis and colleagues [50].

Thus, Kruse and colleagues [51] have developed a mutagenesis-based approach to increase H^+ and e^- supply to the hydrogenases in anaerobic conditions in order to improve H_2 evolution in *C. reindhardtii*. Initially, they isolated the mutants impaired in state 1-to-state 2 transition (e.g., *stm6* [51]) that were locked in linear photosynthetic electron flow. State transition is a rapid regulatory mechanism of balancing photosynthetic electron flow under fluctuating light which in *Chlamydomonas* is also associated with induction of cyclic electron flow around PSI upon overreduction of the plastoquinone pool [52]. As an example of such mutant, *stm6* was not only blocked in cyclic electron flow, but also exhibited excessive starch accumulation, and increased O_2 consumption (due to photofermentation of starch and upregulation of alternative oxidase activity) [51]. All these factors activated endogenous hydrogenase to catalyze molecular hydrogen production, whilst minimizing O_2-induced irreversible inactivation of this enzyme. The reported hydrogen production rates of *stm6* were over 10-fold higher compared to wild type, with ~540 ml of H_2 produced per liter culture over 10–14 days at a maximal rate of 4 ml per hour [51]. More recently, the same group reported another mutant [53] with the truncated light harvesting antenna of PSII, the LHCII system. This mutant exhibited even higher H_2 production rates compared to *stm6* due to better penetration of light into the dense culture inside the bioreactor and minimization of solar energy conversion losses due to the diminished non-photochemical quenching and photoinhibition in this LHCII-depleted mutant under increased light intensities promoting biomass production [53]. Therefore, truncation

of the LHCII antenna results in balancing the rate of photosynthetic O_2 production with the rate of respiration-based O_2 consumption. This in turn facilitates rapid induction of endogenous hydrogenase allowing for the continuous photobiological H_2 production using reducing equivalents produced by PSII from water [53].

PHOTANOL AND PHOTOALCOHOLS. Several model cyanobacterial species have been used as "biosolar cell factories" [54] for metabolic engineering by combining photosynthetic and fermentation pathways using C_3 sugars (glyceraldehyde-3-phosphate and pyruvate) as the central linking intermediates. These include *Synechocystis* sp. PCC 6803, *Synechococcus elongatus* sp. PCC 7492, *Synechococcus* sp. PCC 7002 and *Anabaena* sp. PCC 7120 [55]. To this end, the given fermentation pathways have been metabolically engineered into the cyanobacterial phototrophic metabolism by inserting the appropriate gene cassettes encoding heterologous enzymes required for conversion of photosynthetically produced C_3 sugars into the particular fermentation end product [55,56]. Thus, photofermentative pathways engineered in cyanobacteria resulted in the production of various short-chain alcohols as the end products including isobutanol, 2,3-butanediol, lactate, and ethanol (photanol) [55,57,58]. Of all these HVPs the highest yield for a direct solar-to-biofuel conversion was thus far obtained for synthesis of ethanol (at a rate of 212 mg/l/day) by genetic engineering of heterologous pyruvate decarboxylase from *Zymomonas mobilis* and overexpressing homologous alcohol dehydrogenase in *Synechocystis* sp. PCC6803 [58]. The main challenge of the metabolic engineering approach is to re-direct the great majority of the fixed carbon from biomass into the desired energy product. A promising strategy towards this goal is to remove carbon sinks, e.g., those employed for the storage compounds polyhydroxybutyrate and glycogen [59].

BIODIESEL. Biodiesel is an environmentally friendly, non-toxic biodegradable fuel with low CO_2 emissions obtained from various feedstocks, including oleaginous plants, microalgae and animal fat [60–63]. It consists of methyl esters of long-chain (C_{12}-C_{18}) fatty acids derived from triglycerides that are present in biological feedstocks. As an example, soybean oil is principally employed for biodiesel production in the USA, illustrating at the same time the global "food vs. fuel" problem, i.e., competition for arable land and water supplies as a result of crop-based biodiesel production [2,62]. In this context, the use of microalgae for biodiesel production provides an attractive option as cultivating algae in minimal nutrient requirements does not exert pressure on arable land or water supplies, it can be scaled up and it is not subjected to seasonal fluctuations of solar-to-biomas conversion efficiency. There are numerous examples of microalgae used for biodiesel production including the genera *Botryococcus*, *Chlorella*, *Scenedesmus*, *Chlamydomonas*, *Dunuliella*, and *Nannochloropsis* ([60] and references therein).

The other obvious advantages of using microalgae for conversion of their biomass to biodiesel are their high growth rate and often high lipid content. Importantly for the high combustion quality of algae-derived biodiesel, the lipids synthesized by microalgae upon exposure to environmental stress factors contain mainly neutral fatty acids of a low degree of unsaturation, making algal biodiesel suitable for partial replacement for fossil diesel [61–63].

METHANE. An alternative to reduce climate-associated emissions could be methane and photocatalytic methanol production using CO_2 captured from coal-fired power stations [64]. Under anoxic conditions, biomass can be converted to CH_4 through a process referred to as anaerobic digestion (AD). This process allows for the remaining material after lipid extraction from cyanobacterial biomass to be converted into CH_4, considerable enhancing the total energy recovery. Apart from decreasing the overall costs of the process for bioenergy production, this might lead to a more favorable or positive energetic balance of the overall cyanobacterial biofuel production. Moreover, the oil recovery results in a 21% of the energetic value when the algae accumulate less than 40% of lipids, despite the fact that the energetic costs of lipid recovery involved are higher than 30% [65]. AD thus could represent a good choice for total energetic recovery of biomass. Unfortunately, the research on the matter is quite limited, particularly for CH_4 production by cyanobacterial biomass. Because of this lack of information in the literature it is quite challenging to compare the yield of different cyanobacterial strains. Economically speaking, cyanobacterial methane production is not viable compared to methane derived from fossil fuels. If the current technology is made more cost-effective in the upcoming years the situation might change. Needless to say, the process of methane production by itself or in conjunction to other bioenergy producing processes needs more investment in research [66].

Artificial photosynthesis: a multidisciplinary approach to produce solar fuels

The translation of fundamental mechanistic knowledge, which has been tremendously advanced in recent years from the X-ray crystallographic and state-of-the-art biophysical studies of PSII and PSI, into man-made solar-to-fuel devices is an ongoing key aspect of the artificial photosynthesis research. The main scientific challenge in these endeavors is to construct an "artificial leaf" capable of efficient capturing and conversion of solar energy into chemical bonds of a high-energy density liquid fuel (such as gasoline, kerosene, formate, methanol etc.), while simultaneously generating oxygen from splitting water (Fig. 7).

To date, the main focus has been to design and synthesize water splitting and proton reducing catalysts that can be potentially connected to artificial light-driven charge separation RCs [67]. Various organic dyes have been employed for the latter (e.g. porphyrins, Zn-chlorins, perylenes) [68,69], whereas inorganic semiconductors (e.g., WO_3, TiO_2, Fe_2O_3) are currently the material of choice to split water or power reductive chemistry within the photoelectrochemical cells (Fig. 8) [4,70].

One of the greatest challenges in this field is nanoengineering of suitable semiconductors to efficiently transfer the captured energy of sunlight into multi-electron reduction reactions that are required to convert CO_2 into fuels. The other major challenge is to efficiently interface stable molecular catalysts with these semiconductors that would

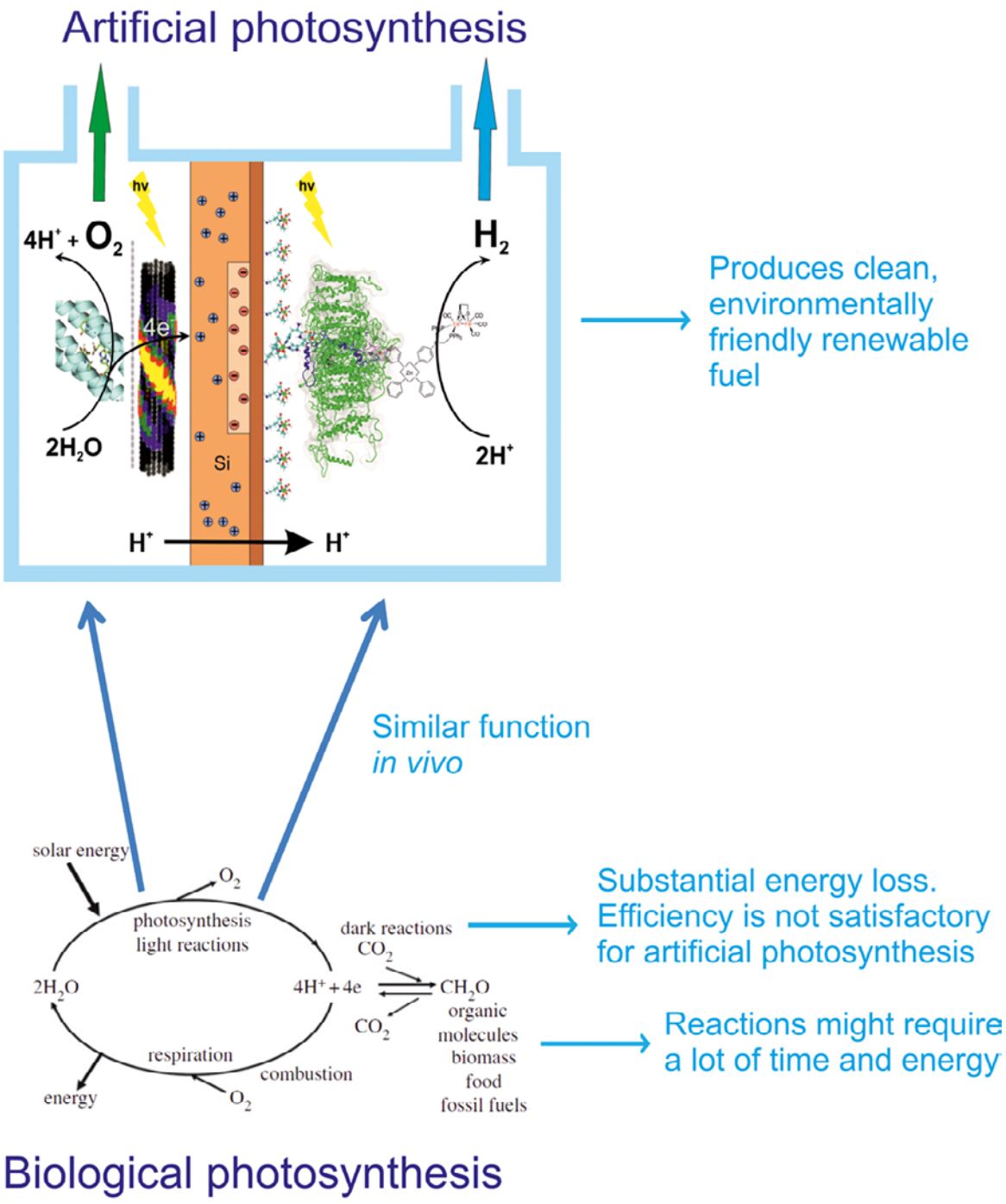

Fig. 7 Artificial versus natural photosynthesis. A comparison between photosynthesis in vivo and artificial photosynthesis explains why it is more energetically viable to employ artificial photosynthesis for clean fuel production. Natural photosynthesis is very inefficient in terms of solar-to-biomass conversion. Artificial photosynthesis short-circuits the natural process by utilizing the most energetically efficient primary events of light capture, charge separation and charge transfer. Lower panel of $H_2/O_2/H_2O$ cycle driven by solar light is reproduced with permission from Barber and Tran [4].

efficiently split water and reduce water-derived protons upon absorption of visible light, as do the natural photosystems. There has been an explosion of reports describing novel synthetic molecular catalysts, some of which are characterized by high turn-over numbers (TON) and turn-over frequencies (TOF), in some cases matching or exceeding those of the natural photosystems. As an example of some of the most remarkable advances in this field is a rationally designed Ru-based catalyst with a TOF of 300 s^{-1}, which is comparable with that of PSII [71]. Another spectacular catalysts for water splitting are based on a relatively abundant element, cobalt. Kanan and Nocera have reported a cheap self-assembling catalyst composed of Co-oxo-borate or phosphate complexes [72,73], which can efficiently split water with a low overpotential at neutral pH, similar to the OEC of PSII. Remarkably, the Co-oxo-phosphate catalyst

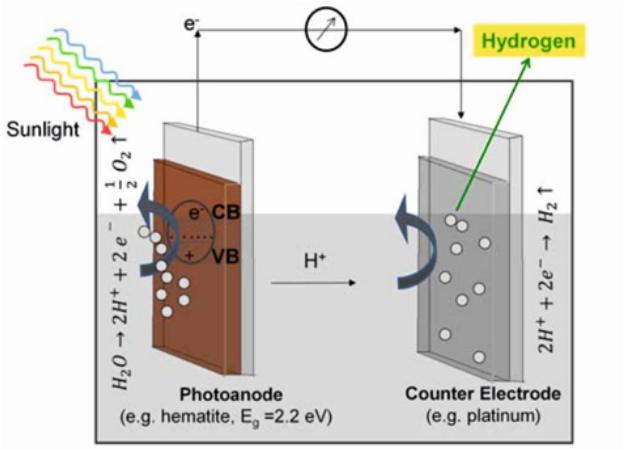

Fig. 8 Principles of the water-splitting and hydrogen-evolving photoelectrochemical cell. Light induces a charge separation within the semiconductor photoanode (CB – conduction band; VB – valence band), and this leads to photocatalytic water splitting into H^+, molecular oxygen and electrons. The protons migrate to the counter electrode (cathode) where they are reduced to H_2 with the photogenerated electrons. In the majority of PEC cells, a certain external overpotential (bias) of 0.5–1 mV needs to be applied in order reach significant H_2 production rates. Figure reproduced with permission from Ihssen et al. [70].

adopts a cubane-like structure, which is very similar to the OEC of PSII [74]. Many more water splitting and hydrogen evolving synthetic catalysts have been reported that have promising TON and TOF numbers. These are overviewed in several excellent recent reviews [4,75–78] and are beyond the scope of the present review.

The advantage of solar-to-H_2 conversion is that molecular hydrogen can be utilized directly as a fuel but can also be employed to reduce CO_2 to simple carbon-based fuels (e.g., methane, methanol, formic acid or carbon monoxide) as molecular precursors for higher molecular weight carbon compounds [76–78]. Efforts to generate high-energy carbon containing fuels, such as methanol, have been made, although progress in the field is rather slow due to the technical challenges associated with the multi-electron character of the CO_2 reduction, as opposed to a single-step reduction of protons into molecular hydrogen. However, the biggest challenge is to functionally integrate robust and highly active individual components (photocatalysts, light harvesting antenna and photoelectrodes) into a complete device operating at high solar power conversion efficiencies in which water splitting and hydrogen production are spatially and temporarily separated. To this end, several exciting advances have been made over the last 3 years that have started turning this highly ambitious goal into realistic technology. These are overviewed below.

Recent advances in biomimetic solar-to-fuel devices

Among various semiconducting substrates used for engineering of artificial leaves hematite (α-Fe_2O_3) has recently become the material of choice for photoanodes due to its inherent material characteristics, such as low cost, environmentally benign nature, corrosion resistance over a wide pH range (and particularly robustness towards photocorrosion), its narrow band gap (2.1 eV), and importantly, its photocatalytic activity in the visible part of the spectrum (approximately 40% solar light is absorbed by this n-type semiconductor) [79]. Many consider hematite essential and even critical for improvement of power conversion efficiency in an artificial leaf, hence, its bulk and surface electronic properties have been investigated in depth for many decades [79]. Recently, a novel photoanode heterostructure of n-type hematite and p-type NiO/α-$Ni(OH)_2$ has been reported by Bora et al. [80] which is particularly efficient in terms of solar energy conversion. This pn-type water-splitting heterojunction assembly was engineered in order to lower bias potential and to maximize current density to overcome the kinetic barrier of the water oxidation reaction. Indeed, such a heterojunction system exhibited an impressive current density which was several times higher than that of pristine hematite film (at 16 mA/cm^2), with the oxidized $Ni(OH)_2$ layer producing the sudden increase in current density [80]. Furthermore, once exposed to AM 1.5 (standard solar illumination) the system displayed charge-storing capacity, along with electrochromic behavior. This is not present in the case of pn-junction-like devices made by mere deposition of NiO on hematite by simple thermal annealing. Moreover, no such behavior was observed for hematite alone. In this way, this novel type of electrode offers a simple low-cost option for both water splitting and charge storage [80]. A related approach features an electron hole doped film in the α-Fe_2O_3 photoanode upon electrochemical oxidation [81].

In contrast to such a fully synthetic water-splitting photoanode, Kargul and colleagues very recently described the successful nanoengineering of nanocrystalline hematite/FTO with the robust red algal PSI-LHCI supercomplex, thus forming a truly green biohybrid photoanode (Fig. 9) [37]. The individual synthetic and biological photoactive components were interfaced to construct a highly organized biophotoanode, which was subsequently used for assembly of the biohybrid dye-sensitized solar cell (DSSC) using Pt counter electrode for reduction of water-derived protons [37]. Electron microscopy and X-ray diffraction analyses showed that red algal PSI-LHCI was immobilized as a structured multilayer over highly ordered nanocrystalline arrays of hematite. Compared to a related tandem system based on TiO_2/PSI-LHCI material (unpublished), the α-Fe_2O_3/PSI-LHCI biophotoanode generated the largest open circuit photocurrent and operated at the highest power conversion efficiency due to a better electronic tuning between the PSI layer and the conductive band of hematite [37]. The nanostructuring of the PS-LHCI multilayer in which the subsequent layers of PSI were organized in the head-to-tail orientation was accomplished by surface charge manipulation at various pH, which enabled immobilization of the PSI-LHCI complex with its reducing side towards the hematite surface [37]. Importantly, upon illumination with visible light above 590 nm, the biohybrid PSI-LHCI-DSSC was capable of sustained photoelectrochemical H_2 production at a rate of 744 μmoles H_2/mg Chl/h, representing one of the best performing biohybrid "green" solar-to-fuel nanodevices capable of sustained H_2 production under standard solar illumination [37].

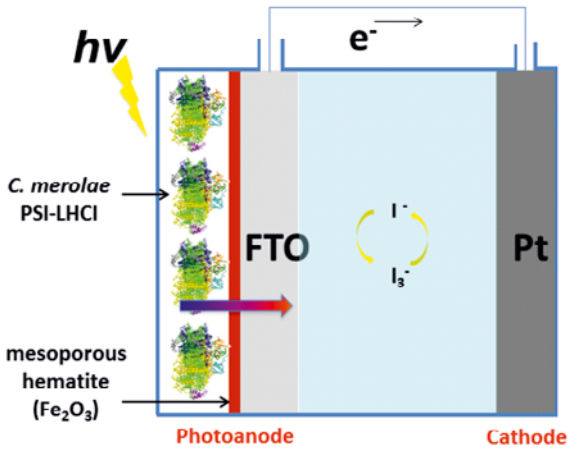

Fig. 9 Diagrammatic representation of biohybrid PSI-based DSSC incorporating photosystem I from a red microalga *Cyanidioschyzon merolae*. Ultrastable red algal PSI-LHCI was nanostructured in head-to-tail oriented multilayer over hematite/FTO electrode [37]. In this way, PSI acts as an efficient photosensitizer/charge separator for hematite, allowing this substrate to split water upon absorption of red/far red light and generate a photocurrent density of up to 57 μA/cm^2. The protons derived from water are reduced on the Pt counter electrode to molecular hydrogen that is sustainably produced by this assembly under standard red-shifted solar illumination.

Braun and colleagues have recently demonstrated a promising strategy for enhancing photocurrent density on semiconductor substrates using other rather simpler in structure light harvesting proteins. Low-cost biomaterials such as cyanobacterial phycocyanin [82] and enzymatically produced melanin [70] were both employed to functionalize electrode surfaces constructed with hematite, thus increasing the overall performance of such cheap metal oxide photoanodes in a biohybrid PEC system. The overall stability and performance of such biohybrid photoanode assemblies was further improved by application of environmentally benign and pH-neutral electrolyte systems [70,82].

Imitating the Z scheme in an artificial leaf

An important benchmark in the quest for a fully operational viable artificial leaf has been very recently provided by the biohybrid approach using natural photosystems for construction of anodic and cathodic half-cells within PEC devices. As overviewed above, PSII and PSI are very efficient as electron generators for the reduction of protons, due to their high quantum efficiency of solar conversion to charge separation, and especially as their substrates are only water and visible light. Photocatalytic properties of photosystems such as the light-driven water splitting conducted by PSII and generation of reducing power by PSI make them the invaluable candidates for the development of semi-artificial devices which convert light energy into stable HVPs such as molecular hydrogen and simple carbon-based fuels [16,18,36].

Recently, an elegant proof-of-concept approach to serially couple PSII and PSI with an Au electrode has yielded one of the first operational semi-artificial PECs producing photocurrents so as to imitate the Z scheme of natural photosynthesis (Fig. 10) [83]. This full Z-scheme mimic resulted in the PEC device in which the two electrochemical half-cells were separated by the Au electrode with PSII or PSI on either side smarty interfaced by the two types of redox compatible osmium complex hydrogel to facilitate direct electron transfer. In this way, the complete biohybrid PEC made a significant advance to previous studies by the same group on construction of individual PSII- and PSI-based half cells [84,85]. Importantly, in contrast to these previous studies the complete photovoltaic cell operated as a closed circuit without any sacrificial electron donors or mediators, using water and solar light as the only substrates [83].

Overall, such serial coupling of two independent processes of light capturing by PSII and PSI in two separate interconnected compartments yielded a fully autonomous biophotovoltaic cell, albeit operating at very low power conversion efficiency. This type of cell is different from previously published biophotovoltaic devices utilising PSI as a photosensitizing light harvesting/charge separating

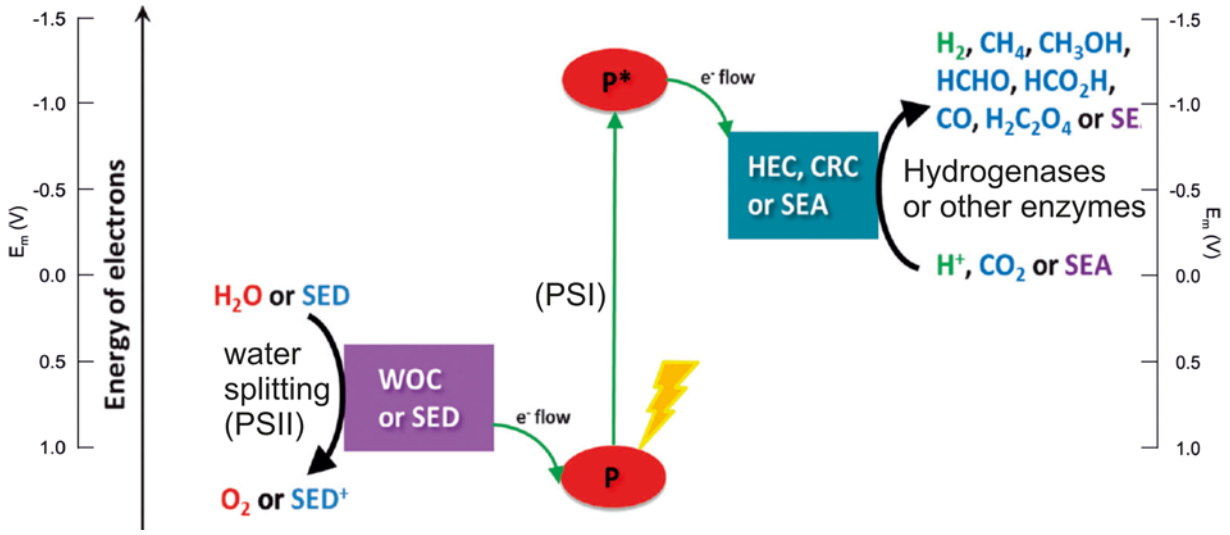

Fig. 10 Reconstruction of the photosynthetic Z scheme in biohybrid solar-to-HVP devices. Diagrammatic representation of artificial photosynthesis. Light converting modules (P), water oxidation catalyst (WOC), sacrificial electron donor (SED), hydrogen evolving catalyst (HEC), CO_2 reduction catalyst (CRC), sacrificial electron acceptor (SEA). Adapted from Berardi et al. [16].

photoanodic component [37,86] as it provides the blueprint for the potential application of such a "biobattery" in conjunction with various synthetic and biological catalysts, since the photoactivated electrons originating from water splitting may be employed for chemical energy conversion rather than reducing oxygen by methyl viologen (as in the case of the Kothe et al. assembly [83]). Of course, PSI has been used in numerous studies as the cathodic component of the H_2-producing half-cell devices, yet all of such devices required an artificial electron donor and metal/hydrogenase catalysts to operate [18,36]. The separation of the oxygen evolving PSII photoanode from the PSI photocathode opens up the possibility to couple PSI with oxygen-sensitive enzymes of HVP pathways such as nitrogenases, CO_2 dehydrogenases or hydrogenases [16,87], as shown schematically in Fig. 10. However, in such prospective assemblies, PSII will likely have to be replaced by a more robust, ideally self-renewing molecular water splitting catalyst to bypass the problem of PSII degradation.

In a similar approach which also utilizes redox-active polymers, Yehezkeli et al. [88] employed polyN,N′-dibenzyl-4,4′-bipyridinium (poly-benzyl viologen, PBV^{2+}) which was employed as the smart matrix for nanostructured assemblies of PSI and/or PSII layers, deposited on indium tin oxide (ITO) electrodes (Fig. 11). As expected, the PSII-functionalized electrode evolved oxygen producing an anodic photocurrent upon illumination with visible light, without the necessity of an artificial electron donor/mediator. In contrast, the layered assembly of PSI generated a cathodic photocurrent only in the presence of a sacrificial electron donor/mediator system (ascorbate/dichlorophenol indophenol). The photocurrent was generated by electron transfer from PSII to the redox polymer and subsequently to the electrode via the PBV^{2+}. The concomitant evolution of molecular oxygen was accompanied by injection of electrons into the electrode by the charge-separated species. Compared to the anodic photocurrent generated by a PSII-modified electrode, the system composed of a PSII layer assembled on a layer of PSI within the matrix of PBV^{2+} showed a 2-fold higher photocurrent compared to the system engineered with PSII alone, most likely due to better charge separation within the PSII/PSI tandem system [88]. Vectorial electron transfer to the electrode was elegantly demonstrated by further nanoengineering of the two photosystems on the electrode using two different redox polymers better tuned in with the redox properties of the photoactivated photosystems, resulting in further (~6-fold) enhancement in the photocurrent density [88], demonstrating the importance of a rational smart matrix-based design for better overall performance of such biohybrid PEC devices.

Although photooxidation of water has been optimized by Nature by means of water splitting cycle catalyzed by the OEC of PSII, mimicking this energetically demanding reaction in an artificial leaf remains a major challenge, not only in terms of operation at a minimal overpotential, exhibiting high TON and TOF numbers of the water splitting catalyst, but also managing the proton coupled electron transfer during the catalysis. One of the more successful assemblies fulfilling these criteria has been recently reported for the water splitting/H_2 generating hybrid system, in which an inorganic H_2-producing photocatalysts CdS and Rh-doped $Ru/SrTiO_3$:Rh (Rh-doped perovskite titanate) and plant O_2-evolving PSII were functionally coupled and integrated with an inorganic redox system [$Fe(CN)_6^{3-}/Fe(CN)_6^{4-}$] in an aqueous solution [89], yielding both O_2 and H_2 upon illumination with visible light. The overall water splitting achieved under standard solar irradiation and the H_2-production rate of this hybrid system reached the impressive values of 1334 mol O_2/mol PSII/h and 2489 mol H_2/mol PSII/h, respectively. In this hybrid system, PSII particles were self-assembling onto the inorganic photocatalysts' surface and the electron transport from PSII to the synthetic photocatalyst was determined to be the rate-limiting step. Importantly, the biohybrid PSII-perovskite system was characterized by exceptionally high TON for H_2 production (over 3751), without the loss of activity for over 3 hours in direct sunlight. In this way, an autonomous biohybrid operational solar-to-fuel nanodevice of PSII and the perovskite catalyst was generated that used solely water and solar energy as substrates for hydrogen production, as does PSII [89].

Recently, Reisner and colleagues reported a hybrid photoanode consisting of *T. elongatus* PSII particles deposited on a high surface area mesoporous ITO electrode [90]. The particular three-dimensional architecture of this material permits favorable high protein coverage and direct electron transfer from PSII to the mesoporous ITO surface. The authors reported the TOF of water oxidation of 0.18 ±0.04 mol O_2/mol PSII/s and a current density of 1.6 ±0.3 μA/cm^2 [90]. Moreover, the study demonstrated great enhancement in photocurrent density upon addition of two external electron mediators, potassium 1,4-naphthoquinone-2-sulfonate (NQS) and 2,6-dichloro-1,4-benzoquinone (DCBQ), indicating somewhat non-favorable interfacing of PSII with ITO which has to be overcome by the addition of external electron transfer mediators. Furthermore, mechanistic studies show electron transfer from the terminal quinone Q_A in addition to the terminal quinone Q_B to the ITO surface [90], something that does not occur in vivo as only Q_B is involved in electron relay in the thylakoid membrane.

In a follow-up work, the same group reported an improvement of the above biohybrid system by both electrostatic and covalent immobilization of the PSII particles on a self-assembled monolayer (SAM)-modified ITO electrode [91]. Significantly, the directed immobilization of PSII, which placed the terminal quinones (Q_A and Q_B) in close proximity of the ITO surface not only enhanced the current density generated by the assembly but also required much less sample deposition (1.1 pmol PSII) [91]. Moreover, the system resulted in enhanced electronic interfacial communication between the PSII and the ITO surface and an increased stability [91] compared to the previous study [90]. Addition of external electron mediators resulted in no significant increase of photocurrent density upon illumination, suggesting that the proximity of the terminal quinones with the ITO surface was good enough for an optimal electron transfer. The work is an excellent proof-of-concept example illustrating that the oriented immobilization of photosynthetic modules with the appropriate electrode is a prerequisite for enhanced direct electron transfer and improved robustness of the biohybrid PEC system.

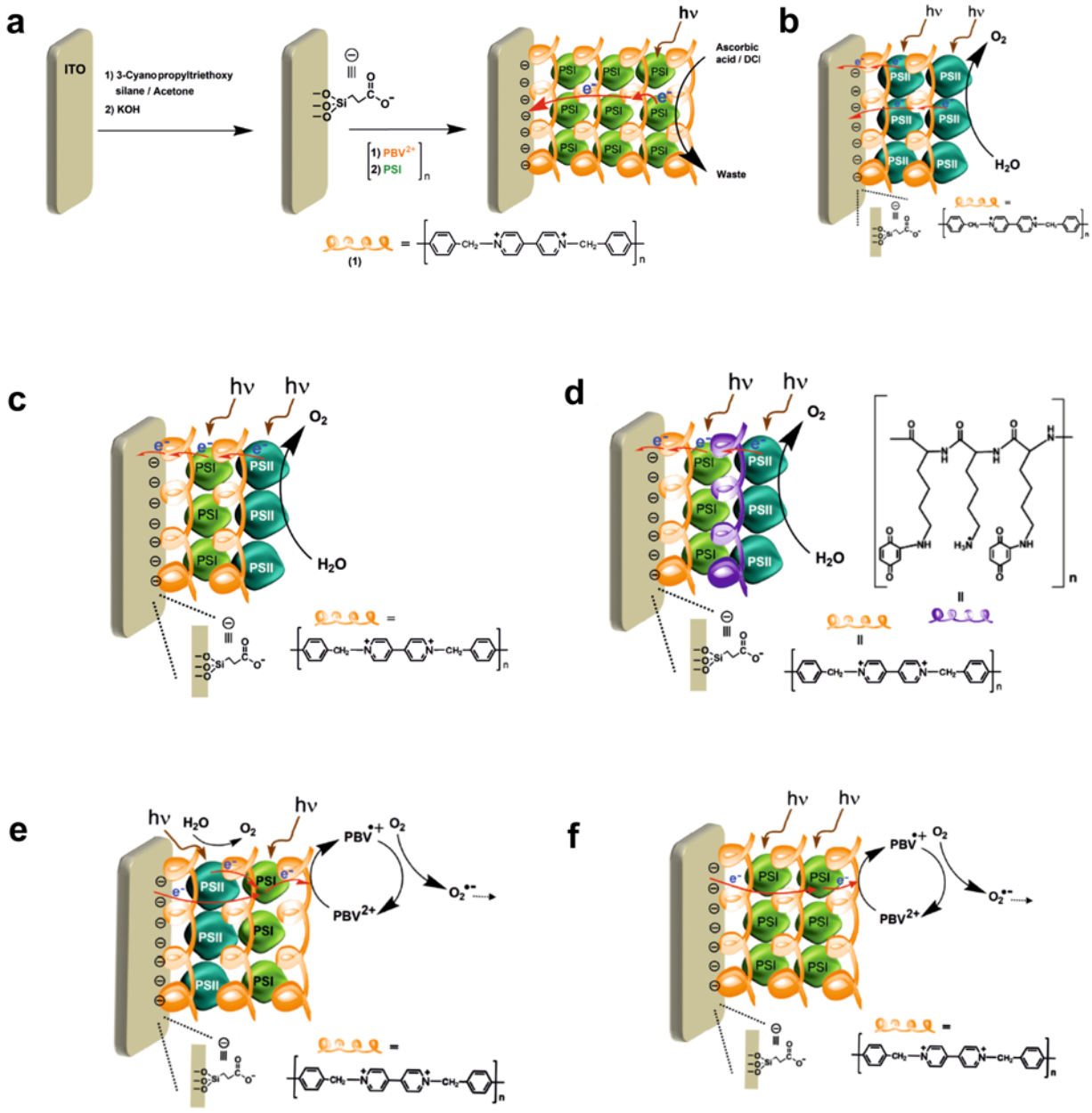

Fig. 11 Nanoengineering the PSII/PSI photoelectrodes using redox active polymers as the smart matrix. Various organizations of PSI and PSII layers redox coupled to each other and/or the electrode surface according to Yehezkeli et al. [88]. **a** Diagrammatic synthesis of the layered PBV^{2+}/PSI photoactive conjunction on the ITO electrode. **b** Diagrammatic assembly of the layered PBV^{2+}/PSII photoactive conjunction on an ITO electrode. **c** Diagrammatic assembly of the layered PBV^{2+}/PSI/PBV^{2+}/PSII photoactive conjunction deposited on an ITO electrode. **d** Diagrammatic assembly of the layered PBV^{2+}/PSI/PBQ/PSII photoactive conjunction on an ITO electrode. **e** Diagrammatic assembly of the layered PSII/PBV^{2+}/PSI photoactive conjunction deposited on an ITO electrode. **f** Diagrammatic representation of the assembly composed of the layered PSI/PBV^{2+}/PSI photoactive conjunction deposited on an ITO electrode. Structures of the interfacing matrices are also shown. Reproduced with permission from Yehezkeli et al. [88].

An interesting approach in the construction of the bio-hybrid H_2-producing nanodevices is based on application of nanostructured hollow nanospheres sized in the optical range and composed of Pt-doped carbon nitride organic semiconductor exhibiting both water splitting or proton reduction activity [92]. These small, hollow semiconducting nanospheres (Fig. 12) function not only as nanostructured scaffold for the Pt co-catalyst but also as the light-harvesting antennae that facilitate photoreduction catalysis. Significantly, such sophisticated highly nanostructured assemblies of optimized thickness have been shown to operate at an impressive solar-to-hydrogen quantum efficiency of 7.5% [92]. Hollow polymerized nanospheres with controlled surface functionalities and shell thickness provide an important

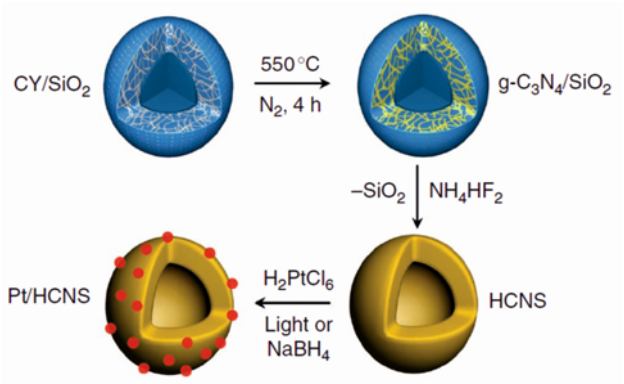

Fig. 12 Synthetic scheme of nanosphere synthesis. A schematic diagrammatic illustration of the hollow carbon nitride nanosphere (HCNS) and Pt co-catalyst/HCNS nanosphere, highlighting the chemical synthesis pathway. This light-harvesting nanosphere of the precisely controlled thickness serves as a photocatalytically active scaffold for immobilization of the metal co-catalyst resulting in both water splitting and molecular hydrogen production under visible light illumination and reaching a solar-to-hydrogen quantum efficiency of 7.5%. Reproduced with permission from Sun et al. [92].

development in artificial photosynthesis field as they can act as a platform for assembling various functionalities into complex nanostructures, while at the same time maintaining "interior" and "exterior" compartments, with a "membrane" separating both of them. In natural photosynthesis, the equivalent of such nanospheres is represented by the thylakoid membrane, where both the water-oxidation catalyst (PSII) and reduction center (PSI) are spatially separated and ordered in tandem for highly efficient energy transfer and photoconversion within the nanosized structures of the reaction centers [5,93].

Recently, Zhou et al. [94] reported a unique design strategy for solar-to-fuel conversion using a real leaf's three-dimensional hierarchical matrix for immobilization of nanostructured crystalline perovskite titanate clusters ($ATiO_3$, with A being Sr, Ca, and Pb) acting as catalysts for both water splitting and photoreduction of CO_2 into simple hydrocarbons (CH_4 and CO). This novel approach allowed for highly efficient, improved gas diffusion and light harvesting within such a photocatalytical semi-artificial system, in an analogous fashion to a well-defined leaf anatomy and physiology. Remarkably, the system operated with no external bias potential (Fig. 13) for water splitting, whilst the solar-to-hydrocarbon quantum yield was further improved by doping with the Au co-catalyst acting as the electron reservoir and

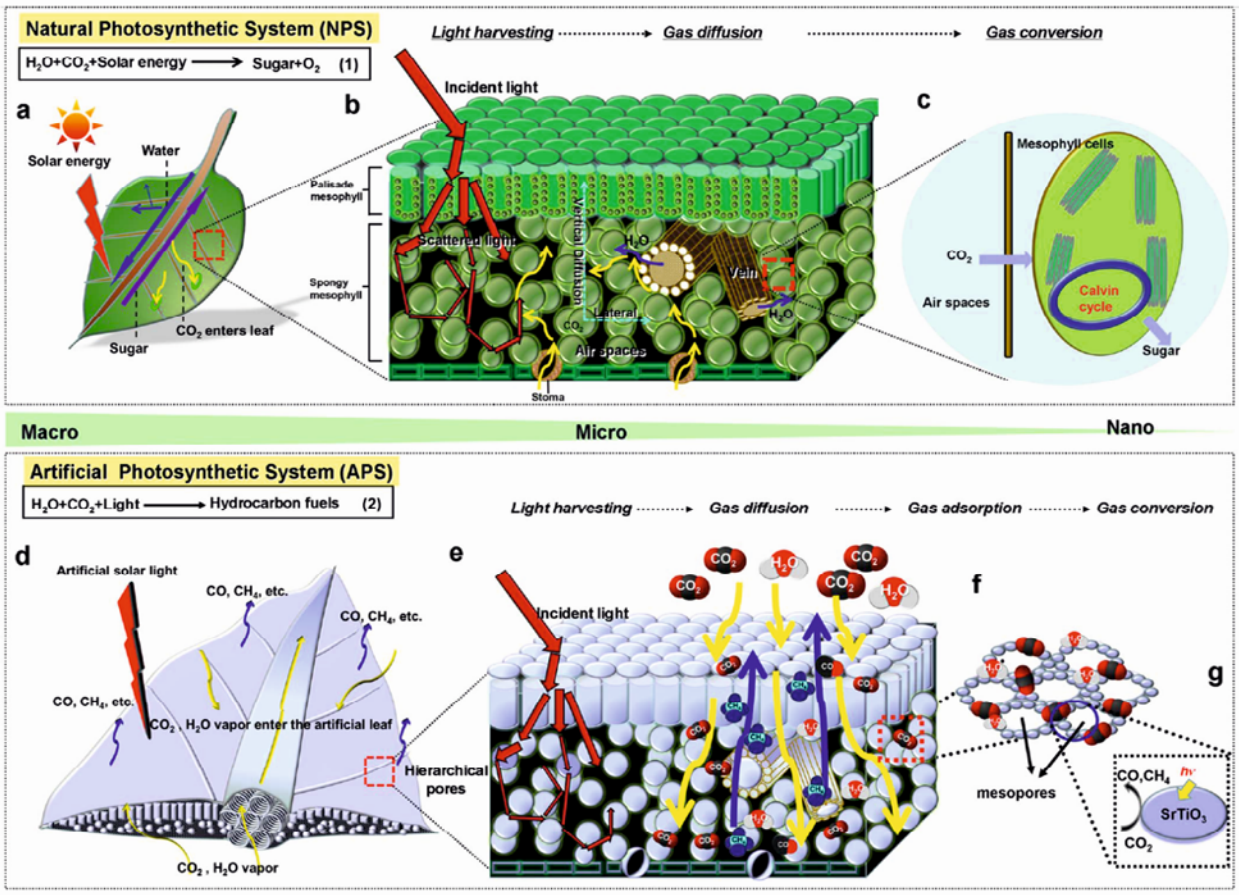

Fig. 13 Schematic diagrammatic illustration and comparison of the essential processes in natural photosynthetic system (NPS) and artificial photosynthetic system (APS). **a** Essential process of photosynthesis in NPS in the leaf. **b** Gas diffusion and light harvesting processes in NPS at the mesophyllic level. **c** Process of gas conversion in mesophyll cells at the chloroplastic level. **d** Artificial photosynthesis basic process in APS at the "artificial leaf" scale. **e** Gas diffusion and light harvesting processes in APS at the mesophyllic level. **f** Process of gas adsorption in APS at the supramolecular level. **g** Processs of gas conversion in APS at the molecular level. Reproduced with permission from Zhou et al. [94].

facilitating proton-coupled electron transfer [94]. The authors postulate that this approach may be extended to construction of other 3D scaffolds with other interesting multi-metallic oxides, such as niobates (e.g. $NaNbO_3$) or tantalates (e.g. $NaTaO_3$, $KTaO_3$, $Sr_2Ta_2O_7$) [94]. Moreover, this approach may also be applied to polymeric metal-free photocatalysts (e.g., graphitic carbon nitride) based on earth-abundant elements. This is the first example that employs leaf architecture as a scaffold for the nanoengineering of artificial leaves for CO_2 photoreduction, and thus in our view, represents a major breakthrough in the field of artificial photosynthesis.

Conclusions and future outlook

The inherent depletion of fossil fuels and relying entirely on the use of fossil fuels to power our economies must be skillfully addressed in the coming years to sustain economic growth. An attractive alternative to burning fossil fuels is provided through introduction of carbon-neutral, transportable energy carriers made from renewable resources. To date, biomass-based fuels are still quite restricted in terms of scale and their production remains controversial in many cases mainly due to the "food or fuel" problem. The limitation is global, and unfortunately the scale of fossil and biomass-based fuels cannot be compared, with the latter being present on our planet in much lesser quantities. Moreover, when the energy demand will grow in the not-too-distant future, from the current annual use of 16 TW to projected 50 TW by 2100 [1], the situation is likely to worsen. As mentioned previously, solar energy seems to be the most abundant source of renewable energy available on our planet. The terms "solar fuel" and "artificial leaf" have become well established within the scientific community seeking to provide clean, green alternatives to fossil fuels for energy production.

In order to be able to adapt solar energy on a global scale, scientific breakthroughs must demonstrate that this is a viable technology, i.e., the energy must be harnessed, stored and used at the maximum possible efficiency, whilst minimizing energy losses or unwanted back reactions. In contrast to other renewable energy sources there is more than enough of solar energy falling on Earth each hour to meet global energy demand of mankind for an entire year. Therefore, transition from fossil fuel-based economies to this renewable practically limitless energy source, even at modest power conversion efficiencies seems the only viable option for generation of solar fuels or photocurrents in long term. It is also important to emphasize that in order to maximize the efficiency of solar energy conversion, the energy ideally should be stored in the form of high energy density liquid fuels. Realistically, the efficiency target for "artificial leaves" discussed in this review must reach 10 per cent or better in order to compete with traditional fossil fuel-based technologies of energy production and to fulfill the need of realistic alternative technologies addressing the increasing global energy demand. Smart matrix engineering seems to be the key aspect towards this goal, whereby intelligent nanoengineering of robust catalytic and light harvesting modules together with charge separation modules and management of proton relay network is skillfully applied to produce fully integrated working devices that produce fuel from water upon capture of solar energy. Just as the leaf does…

Acknowledgments

JDJO and JK are grateful for the support of the Polish Ministry of Science and Higher Education and the European Science Foundation (grant No. 844/N-ESF EuroSolarFuels/10/2011/0 to JK) and all the fruitful collaborations within the EUROCORES/EuroSolarFuels/Solarfueltandem network. JDJO is supported by the PRELUDIUM grant awarded by the Polish National Science Center (grant No. UMO-2013/11/N/NZ1/02390 to JDJO).

Authors' contributions

The following declarations about authors' contributions to the research have been made: co-wrote the article and prepared the majority of the figures: JDJO; co-wrote, revised the article and prepared some figures: JK.

Competing interests

No competing interests have been declared.

References

1. Shafiee S, Topal E. When will fossil fuel reserves be diminished? Energy Policy. 2009;37(1):181–189. http://dx.doi.org/10.1016/j.enpol.2008.08.016
2. Stephens E, Ross IL, Mussgnug JH, Wagner LD, Borowitzka MA, Posten C, et al. Future prospects of microalgal biofuel production systems. Trends Plant Sci. 2010;15(10):554–564. http://dx.doi.org/10.1016/j.tplants.2010.06.003
3. Industries [Internet]. Shell global. 2014 [cited 2014 Sep 9]; Available from: http://www.shell.com/global/products-services/solutions-for-businesses/lubes/industries.html
4. Barber J, Tran PD. From natural to artificial photosynthesis. Interface Focus. 2013;10(81):20120984. http://dx.doi.org/10.1098/rsif.2012.0984
5. Kargul J, Barber J. Structure and function of photosynthetic reaction centres. In: Wydrzynski TJ, Hillier W, editors. Molecular solar fuels. Cambridge: Royal Society of Chemistry; 2011. p. 107–142. http://dx.doi.org/10.1039/9781849733038-00107
6. Larkum AWD. Evolution of the reaction centers and photosystems. In: Renger G, editor. Primary processes of photosynthesis: principles and apparatus. Cambridge: Royal Society of Chemistry; 2008. p. 489–521.
7. Barber J. Engine of life and big bang of evolution: a personal perspective. Photosynth Res. 2004;80(1–3):137–155. http://dx.doi.org/10.1023/B:PRES.0000030662.04618.27
8. Hohmann-Marriott MF, Blankenship RE. Evolution of photosynthesis. Annu Rev Plant Biol. 2011;62(1):515–548. http://dx.doi.org/10.1146/annurev-arplant-042110-103811
9. Hurles M. Gene duplication: the genomic trade in spare parts. PLoS Biol. 2004;2(7):e206. http://dx.doi.org/10.1371/journal.pbio.0020206
10. Pennisi E. Genome duplications: the stuff of evolution? Science. 2001;294(5551):2458–2460. http://dx.doi.org/10.1126/science.294.5551.2458
11. Raymond J, Blankenship RE. Horizontal gene transfer in eukaryotic algal evolution. Proc Natl Acad Sci USA. 2003;100(13):7419–7420. http://dx.doi.org/10.1073/pnas.1533212100
12. Igarashi N, Harada J, Nagashima S, Matsuura K, Shimada K, Nagashima KV. Horizontal transfer of the photosynthesis gene cluster and operon rearrangement in purple bacteria. J Mol Evol. 2001;52(4):333–341. http://dx.doi.org/10.1007/s002390010163
13. Sadekar S. Conservation of distantly related membrane proteins: photosynthetic reaction centers share a common structural core. Mol Biol Evol. 2006;23(11):2001–2007. http://dx.doi.org/10.1093/molbev/msl079

14. Murray JW, Duncan J, Barber J. CP43-like chlorophyll binding proteins: structural and evolutionary implications. Trends Plant Sci. 2006;11(3):152–158. http://dx.doi.org/10.1016/j.tplants.2006.01.007
15. Blankenship RE, Tiede DM, Barber J, Brudvig GW, Fleming G, Ghirardi M, et al. Comparing photosynthetic and photovoltaic efficiencies and recognizing the potential for improvement. Science. 2011;332(6031):805–809. http://dx.doi.org/10.1126/science.1200165
16. Berardi S, Drouet S, Francàs L, Gimbert-Suriñach C, Guttentag M, Richmond C, et al. Molecular artificial photosynthesis. Chem Soc Rev. 2014;43(22):7501–7519. http://dx.doi.org/10.1039/C3CS60405E
17. Field CB. Primary production of the biosphere: integrating terrestrial and oceanic components. Science. 1998;281(5374):237–240. http://dx.doi.org/10.1126/science.281.5374.237
18. Kargul J, Janna Olmos JD, Krupnik T. Structure and function of photosystem I and its application in biomimetic solar-to-fuel systems. J Plant Physiol. 2012;169(16):1639–1653. http://dx.doi.org/10.1016/j.jplph.2012.05.018
19. Munekage Y, Hashimoto M, Miyake C, Tomizawa KI, Endo T, Tasaka M, et al. Cyclic electron flow around photosystem I is essential for photosynthesis. Nature. 2004;429(6991):579–582. http://dx.doi.org/10.1038/nature02598
20. Johnson GN. Physiology of PSI cyclic electron transport in higher plants. Biochim Biophys Acta. 2011;1807(3):384–389. http://dx.doi.org/10.1016/j.bbabio.2010.11.009
21. Joliot P, Johnson GN. Regulation of cyclic and linear electron flow in higher plants. Proc Natl Acad Sci USA. 2011;108(32):13317–13322. http://dx.doi.org/10.1073/pnas.1110189108
22. Hertle AP, Blunder T, Wunder T, Pesaresi P, Pribil M, Armbruster U, et al. PGRL1 is the elusive ferredoxin-plastoquinone reductase in photosynthetic cyclic electron flow. Mol Cell. 2013;49(3):511–523. http://dx.doi.org/10.1016/j.molcel.2012.11.030
23. DalCorso G, Pesaresi P, Masiero S, Aseeva E, Schünemann D, Finazzi G, et al. A complex containing PGRL1 and PGR5 is involved in the switch between linear and cyclic electron flow in *Arabidopsis*. Cell. 2008;132(2):273–285. http://dx.doi.org/10.1016/j.cell.2007.12.028
24. Peng L, Fukao Y, Fujiwara M, Takami T, Shikanai T. Efficient operation of NAD(P)H dehydrogenase requires supercomplex formation with photosystem I via minor LHCI in *Arabidopsis*. Plant Cell. 2009;21(11):3623–3640. http://dx.doi.org/10.1105/tpc.109.068791
25. Yamori W, Sakata N, Suzuki Y, Shikanai T, Makino A. Cyclic electron flow around photosystem I via chloroplast NAD(P)H dehydrogenase (NDH) complex performs a significant physiological role during photosynthesis and plant growth at low temperature in rice. Plant J. 2011;68(6):966–976. http://dx.doi.org/10.1111/j.1365-313X.2011.04747.x
26. Kukuczka B, Magneschi L, Petroutsos D, Steinbeck J, Bald T, Powikrowska M, et al. Proton gradient regulation5-like1-mediated cyclic electron flow is crucial for acclimation to anoxia and complementary to nonphotochemical quenching in stress adaptation. Plant Physiol. 2014;165(4):1604–1617. http://dx.doi.org/10.1104/pp.114.240648
27. Nelson N, Yocum CF. Structure and function of photosystems I and II. Annu Rev Plant Biol. 2006;57(1):521–565. http://dx.doi.org/10.1146/annurev.arplant.57.032905.105350
28. Cardona T, Sedoud A, Cox N, Rutherford AW. Charge separation in photosystem II: a comparative and evolutionary overview. Biochim Biophys Acta. 2012;1817(1):26–43. http://dx.doi.org/10.1016/j.bbabio.2011.07.012
29. Umena Y, Kawakami K, Shen JR, Kamiya N. Crystal structure of oxygen-evolving photosystem II at a resolution of 1.9 Å. Nature. 2011;473(7345):55–60. http://dx.doi.org/10.1038/nature09913
30. Kanady JS, Tsui EY, Day MW, Agapie T. A synthetic model of the Mn_3Ca subsite of the oxygen-evolving complex in photosystem II. Science. 2011;333(6043):733–736. http://dx.doi.org/10.1126/science.1206036
31. Ananyev G, Dismukes GC. How fast can photosystem II split water? Kinetic performance at high and low frequencies. Photosynth Res. 2005;84(1-3):355–365. http://dx.doi.org/10.1007/s11120-004-7081-1
32. Badura A, Kothe T, Schuhmann W, Rögner M. Wiring photosynthetic enzymes to electrodes. Energy Environ Sci. 2011;4(9):3263. http://dx.doi.org/10.1039/c1ee01285a
33. Jordan P, Fromme P, Witt HT, Klukas O, Saenger W, Krauss N. Three-dimensional structure of cyanobacterial photosystem I at 2.5 A resolution. Nature. 2001;411(6840):909–917. http://dx.doi.org/10.1038/35082000
34. Ben-Shem A, Frolow F, Nelson N. Crystal structure of plant photosystem I. Nature. 2003;426(6967):630–635. http://dx.doi.org/10.1038/nature02200
35. Amunts A, Drory O, Nelson N. The structure of a plant photosystem I supercomplex at 3.4 A resolution. Nature. 2007;447(7140):58–63. http://dx.doi.org/10.1038/nature05687
36. Nguyen K, Bruce BD. Growing green electricity: progress and strategies for use of photosystem I for sustainable photovoltaic energy conversion. Biochim Biophys Acta. 2014;1837(9):1553–1566. http://dx.doi.org/10.1016/j.bbabio.2013.12.013
37. Ocakoglu K, Krupnik T, van den Bosch B, Harputlu E, Gullo MP, Olmos JDJ, et al. Photosystem I-based biophotovoltaics on nanostructured hematite. Adv Funct Mater. 2014 (in press). http://dx.doi.org/10.1002/adfm.201401399
38. Pandey D, Agrawal M. Carbon footprint estimation in the agriculture sector. In: Muthu SS, editor. Assessment of carbon footprint in different industrial sectors. Singapore: Springer; 2014. p. 25–47. (vol 1). http://dx.doi.org/10.1007/978-981-4560-41-2_2
39. Jajesniak P, Ali H, Wong TS. Carbon dioxide capture and utilization using biological systems: opportunities and challenges. J Bioprocess Biotech. 2014;4(155). http://dx.doi.org/10.4172/2155-9821.1000155
40. Zhao B, Su Y. Process effect of microalgal-carbon dioxide fixation and biomass production: a review. Renew Sustain Energy Rev. 2014;31:121–132. http://dx.doi.org/10.1016/j.rser.2013.11.054
41. Oliver JWK, Machado IMP, Yoneda H, Atsumi S. Combinatorial optimization of cyanobacterial 2,3-butanediol production. Metab Eng. 2014;22:76–82. http://dx.doi.org/10.1016/j.ymben.2014.01.001
42. Machado IMP, Atsumi S. Cyanobacterial biofuel production. J Biotech. 2012;162(1):50–56. http://dx.doi.org/10.1016/j.jbiotec.2012.03.005
43. Rabinovitch-Deere CA, Oliver JWK, Rodriguez GM, Atsumi S. Synthetic biology and metabolic engineering approaches to produce biofuels. Chem Rev. 2013;113(7):4611–4632. http://dx.doi.org/10.1021/cr300361t
44. Smith KS, Ferry JG. Prokaryotic carbonic anhydrases. FEMS Microbiol Rev. 2000;24(4):335–366. http://dx.doi.org/10.1111/j.1574-6976.2000.tb00546.x
45. Rosgaard L, de Porcellinis AJ, Jacobsen JH, Frigaard NU, Sakuragi Y. Bioengineering of carbon fixation, biofuels, and biochemicals in cyanobacteria and plants. J Biotech. 2012;162(1):134–147. http://dx.doi.org/10.1016/j.jbiotec.2012.05.006
46. Quintana N, van der Kooy F, Van de Rhee MD, Voshol GP, Verpoorte R. Renewable energy from cyanobacteria: energy production optimization by metabolic pathway engineering. Appl Microbiol Biotechnol. 2011;91(3):471–490. http://dx.doi.org/10.1007/s00253-011-3394-0
47. Das D. Hydrogen production by biological processes: a survey of literature. Int J Hydrog. Energy. 2001;26(1):13–28. http://dx.doi.org/10.1016/S0360-3199(00)00058-6
48. Abed RMM, Dobretsov S, Sudesh K. Applications of cyanobacteria in biotechnology. J Appl Microbiol. 2009;106(1):1–12. http://dx.doi.org/10.1111/j.1365-2672.2008.03918.x
49. Dutta D, De D, Chaudhuri S, Bhattacharya SK. Hydrogen production by cyanobacteria. Microb Cell Fact. 2005;4(1):36. http://dx.doi.org/10.1186/1475-2859-4-36
50. Melis A, Zhang L, Forestier M, Ghirardi M, Seibert M. Sustained photobiological hydrogen gas production upon reversible inactivation of oxygen evolution in the green alga *Chlamydomonas reinhardtii*. Plant Physiol. 2000;122(1):127–136. http://dx.doi.org/10.1104/pp.122.1.127
51. Kruse O, Rupprecht J, Bader K-P, Thomas-Hall S, Schenk PM, Finazzi G, et al. Improved photobiological H_2 production in engineered green algal cells. J Biol Chem. 2005;280(40):34170–34177. http://dx.doi.org/10.1074/jbc.M503840200
52. Kargul J, Barber J. Photosynthetic acclimation: structural

reorganisation of light harvesting antenna - role of redox-dependent phosphorylation of major and minor chlorophyll *a*/*b* binding proteins. FEBS J. 2008;275(6):1056–1068. http://dx.doi.org/10.1111/j.1742-4658.2008.06262.x

53. Oey M, Ross IL, Stephens E, Steinbeck J, Wolf J, Radzun KA, et al. RNAi knock-down of LHCBM1, 2 and 3 increases photosynthetic H_2 production efficiency of the green alga *Chlamydomonas reinhardtii*. PLoS ONE. 2013;8(4):e61375. http://dx.doi.org/10.1371/journal.pone.0061375
54. Angermayr SA, Hellingwerf KJ, Lindblad P, Teixeira de Mattos MJ. Energy biotechnology with cyanobacteria. Curr Opin Biotechnol. 2009;20(3):257–263. http://dx.doi.org/10.1016/j.copbio.2009.05.011
55. Savakis P, Hellingwerf KJ. Engineering cyanobacteria for direct biofuel production from CO_2. Curr Opin Biotechnol. 2015;33:8–14. http://dx.doi.org/10.1016/j.copbio.2014.09.007
56. van der Woude AD, Angermayr SA, Puthan Veetil V, Osnato A, Hellingwerf KJ. Carbon sink removal: increased photosynthetic production of lactic acid by *Synechocystis* sp. PCC6803 in a glycogen storage mutant. J Biotech. 2014;184:100–102. http://dx.doi.org/10.1016/j.jbiotec.2014.04.029
57. Wijffels RH, Kruse O, Hellingwerf KJ. Potential of industrial biotechnology with cyanobacteria and eukaryotic microalgae. Curr Opin Biotechnol. 2013;24(3):405–413. http://dx.doi.org/10.1016/j.copbio.2013.04.004
58. Gao Z, Zhao H, Li Z, Tan X, Lu X. Photosynthetic production of ethanol from carbon dioxide in genetically engineered cyanobacteria. Energy Environ Sci. 2012;5(12):9857. http://dx.doi.org/10.1039/c2ee22675h
59. Qi F, Yao L, Tan X, Lu X. Construction, characterization and application of molecular tools for metabolic engineering of *Synechocystis* sp. Biotechnol Lett. 2013;35(10):1655–1661. http://dx.doi.org/10.1007/s10529-013-1252-0
60. Ho SH, Ye X, Hasunuma T, Chang JS, Kondo A. Perspectives on engineering strategies for improving biofuel production from microalgae – a critical review. Biotechnol Adv. 2014;32(8):1448–1459. http://dx.doi.org/10.1016/j.biotechadv.2014.09.002
61. PC Lai E. Biodiesel: environmental friendly alternative to petrodiesel. J Pet Env. Biotechnol. 2014;5(1). http://dx.doi.org/10.4172/2157-7463.1000e122
62. Ragauskas AME, Ragauskas AJ. Re-defining the future of FOG and biodiesel. J Pet Environ Biotechnol. 2013;4(1). http://dx.doi.org/10.4172/2157-7463.1000e118
63. Talebi AF, Mohtashami SK, Tabatabaei M, Tohidfar M, Bagheri A, Zeinalabedini M, et al. Fatty acids profiling: a selective criterion for screening microalgae strains for biodiesel production. Algal Res. 2013;2(3):258–267. http://dx.doi.org/10.1016/j.algal.2013.04.003
64. Trudewind CA, Schreiber A, Haumann D. Photocatalytic methanol and methane production using captured CO_2 from coal power plants. Part II – well-to-wheel analysis on fuels for passenger transportation services. J Clean Prod. 2014;70:38–49. http://dx.doi.org/10.1016/j.jclepro.2014.02.024
65. Sialve B, Bernet N, Bernard O. Anaerobic digestion of microalgae as a necessary step to make microalgal biodiesel sustainable. Biotechnol Adv. 2009;27(4):409–416. http://dx.doi.org/10.1016/j.biotechadv.2009.03.001
66. Rittmann BE. Opportunities for renewable bioenergy using microorganisms. Biotechnol Bioeng. 2008;100(2):203–212. http://dx.doi.org/10.1002/bit.21875
67. Thapper A, Styring S, Saracco G, Rutherford AW, Robert B, Magnuson A, et al. Artificial photosynthesis for solar fuels – an evolving research field within AMPEA, a joint programme of the european energy research alliance. Green. 2013;3(1):43–57. http://dx.doi.org/10.1515/green-2013-0007
68. Ocakoglu K, Joya KS, Harputlu E, Tarnowska A, Gryko DT. A nanoscale bio-inspired light-harvesting system developed from self-assembled alkyl-functionalized metallochlorin nano-aggregates. Nanoscale. 2014;6(16):9625. http://dx.doi.org/10.1039/C4NR01661K
69. Llansola-Portoles MJ, Bergkamp JJ, Tomlin J, Moore TA, Kodis G, Moore AL, et al. Photoinduced electron transfer in perylene-TiO_2 nanoassemblies. Photochem Photobiol. 2013;89(6):1375–1382. http://dx.doi.org/10.1111/php.12108
70. Ihssen J, Braun A, Faccio G, Gajda-Schrantz K, Thöny-Meyer L. Light harvesting proteins for solar fuel generation in bioengineered photoelectrochemical cells. Curr Protein Pept Sci. 2014;15(4):374–384. http://dx.doi.org/10.2174/1389203715666140327105530
71. Duan L, Bozoglian F, Mandal S, Stewart B, Privalov T, Llobet A, et al. A molecular ruthenium catalyst with water-oxidation activity comparable to that of photosystem II. Nat Chem. 2012;4(5):418–423. http://dx.doi.org/10.1038/nchem.1301
72. Kanan MW, Nocera DG. In situ formation of an oxygen-evolving catalyst in neutral water containing phosphate and Co^{2+}. Science. 2008;321(5892):1072–1075. http://dx.doi.org/10.1126/science.1162018
73. Reece SY, Hamel JA, Sung K, Jarvi TD, Esswein AJ, Pijpers JJH, et al. Wireless solar water splitting using silicon-based semiconductors and earth-abundant catalysts. Science. 2011;334(6056):645–648. http://dx.doi.org/10.1126/science.1209816
74. Kanan MW, Yano J, Surendranath Y, Dincă M, Yachandra VK, Nocera DG. Structure and valency of a cobalt–phosphate water oxidation catalyst determined by in situ X-ray spectroscopy. J Am Chem Soc. 2010;132(39):13692–13701. http://dx.doi.org/10.1021/ja1023767
75. Tran PD, Wong LH, Barber J, Loo JSC. Recent advances in hybrid photocatalysts for solar fuel production. Energy Environ Sci. 2012;5(3):5902. http://dx.doi.org/10.1039/c2ee02849b
76. Bensaid S, Centi G, Garrone E, Perathoner S, Saracco G. Towards artificial leaves for solar hydrogen and fuels from carbon dioxide. ChemSusChem. 2012;5(3):500–521. http://dx.doi.org/10.1002/cssc.201100661
77. Kim JH, Nam DH, Park CB. Nanobiocatalytic assemblies for artificial photosynthesis. Curr Opin Biotechnol. 2014;28:1–9. http://dx.doi.org/10.1016/j.copbio.2013.10.008
78. Benson EE, Kubiak CP, Sathrum AJ, Smieja JM. Electrocatalytic and homogeneous approaches to conversion of CO_2 to liquid fuels. Chem Soc Rev. 2009;38(1):89. http://dx.doi.org/10.1039/b804323j
79. Bora DK, Braun A, Constable EC. "In rust we trust". Hematite – the prospective inorganic backbone for artificial photosynthesis. Energy Environ Sci. 2013;6(2):407–425. http://dx.doi.org/10.1039/C2EE23668K
80. Bora DK, Braun A, Erni R, Müller U, Döbeli M, Constable EC. Hematite–NiO/α-$Ni(OH)_2$ heterostructure photoanodes with high electrocatalytic current density and charge storage capacity. Phys Chem Chem Phys. 2013;15(30):12648. http://dx.doi.org/10.1039/c3cp52179f
81. Gajda-Schrantz K, Tymen S, Boudoire F, Toth R, Bora DK, Calvet W, et al. Formation of an electron hole doped film in the α-Fe_2O_3 photoanode upon electrochemical oxidation. Phys Chem Chem Phys. 2013;15(5):1443. http://dx.doi.org/10.1039/c2cp42597a
82. Bora DK, Rozhkova EA, Schrantz K, Wyss PP, Braun A, Graule T, et al. Functionalization of nanostructured hematite thin-film electrodes with the light-harvesting membrane protein C-phycocyanin yields an enhanced photocurrent. Adv Funct Mater. 2012;22(3):490–502. http://dx.doi.org/10.1002/adfm.201101830
83. Kothe T, Plumeré N, Badura A, Nowaczyk MM, Guschin DA, Rögner M, et al. Combination of a photosystem 1-based photocathode and a photosystem 2-based photoanode to a Z-scheme mimic for biophotovoltaic applications. Angew Chem Int Ed Engl. 2013;52(52):14233–14236. http://dx.doi.org/10.1002/anie.201303671
84. Badura A, Guschin D, Esper B, Kothe T, Neugebauer S, Schuhmann W, et al. Photo-induced electron transfer between photosystem 2 via cross-linked redox hydrogels. Electroanalysis. 2008;20(10):1043–1047. http://dx.doi.org/10.1002/elan.200804191
85. Badura A, Guschin D, Kothe T, Kopczak MJ, Schuhmann W, Rögner M. Photocurrent generation by photosystem 1 integrated in crosslinked redox hydrogels. Energy Environ Sci. 2011;4(7):2435. http://dx.doi.org/10.1039/c1ee01126j
86. Mershin A, Matsumoto K, Kaiser L, Yu D, Vaughn M, Nazeeruddin MK, et al. Self-assembled photosystem-I biophotovoltaics on nanostructured TiO_2 and ZnO. Sci Rep. 2012;2:1–7. http://dx.doi.org/10.1038/srep00234
87. Wenk SO, Qian DJ, Wakayama T, Nakamura C, Zorin N, Rögner M,

et al. Biomolecular device for photoinduced hydrogen production. Int J Hydrog. Energy. 2002;27(11–12):1489–1493. http://dx.doi.org/10.1016/S0360-3199(02)00094-0

88. Yehezkeli O, Tel-Vered R, Michaeli D, Nechushtai R, Willner I. Photosystem I (PSI)/photosystem II (PSII)-based photo-bioelectrochemical cells revealing directional generation of photocurrents. Small. 2013;9(17):2970–2978. http://dx.doi.org/10.1002/smll.201300051
89. Wang W, Chen J, Li C, Tian W. Achieving solar overall water splitting with hybrid photosystems of photosystem II and artificial photocatalysts. Nat Commun. 2014;5:4647. http://dx.doi.org/10.1038/ncomms5647
90. Kato M, Cardona T, Rutherford AW, Reisner E. Photoelectrochemical water oxidation with photosystem II integrated in a mesoporous indium–tin oxide electrode. J Am Chem Soc. 2012;134(20):8332–8335. http://dx.doi.org/10.1021/ja301488d
91. Kato M, Cardona T, Rutherford AW, Reisner E. Covalent immobilization of oriented photosystem II on a nanostructured electrode for solar water oxidation. J Am Chem Soc. 2013;135(29):10610–10613. http://dx.doi.org/10.1021/ja404699h
92. Sun J, Zhang J, Zhang M, Antonietti M, Fu X, Wang X. Bioinspired hollow semiconductor nanospheres as photosynthetic nanoparticles. Nat Commun. 2012;3:1139. http://dx.doi.org/10.1038/ncomms2152
93. Engel GS, Calhoun TR, Read EL, Ahn TK, Mančal T, Cheng YC, et al. Evidence for wavelike energy transfer through quantum coherence in photosynthetic systems. Nature. 2007;446(7137):782–786. http://dx.doi.org/10.1038/nature05678
94. Zhou H, Guo J, Li P, Fan T, Zhang D, Ye J. Leaf-architectured 3D hierarchical artificial photosynthetic system of perovskite titanates towards CO_2 photoreduction into hydrocarbon fuels. Sci Rep. 2013;3:1667. http://dx.doi.org/10.1038/srep01667
95. Larkum AWD. Harvesting solar energy through natural or artificial photosynthesis: scientific, social, political and economic implications. In: Wydrzynski TJ, Hillier W, editors. Molecular solar fuels. Cambridge: Royal Society of Chemistry; 2011. p. 1–19. http://dx.doi.org/10.1039/9781849733038-00001
96. Kato M, Zhang JZ, Paul N, Reisner E. Protein film photoelectrochemistry of the water oxidation enzyme photosystem II. Chem Soc Rev. 2014;43(18):6485. http://dx.doi.org/10.1039/C4CS00031E
97. Redinbo MR, Cascio D, Choukair MK, Rice D, Merchant S, Yeates TO. The 1.5-.ANG. crystal structure of plastocyanin from the green alga *Chlamydomonas reinhardtii*. Biochemistry. 1993;32(40):10560–10567. http://dx.doi.org/10.1021/bi00091a005
98. Kameda H, Hirabayashi K, Wada K, Fukuyama K. Mapping of protein-protein interaction sites in the plant-type [2Fe-2S] ferredoxin. PloS One. 2011;6(7):e21947. http://dx.doi.org/10.1371/journal.pone.0021947